

Aspects of ${}^3\text{He}$ and the Standard Electroweak Model

G.E. Volovik¹

Low Temperature Laboratory,
Helsinki University of Technology
Otakaari 3A, 02150 Espoo, Finland

and

L.D. Landau Institute for Theoretical Physics,
Kosygin Str. 2, 117940 Moscow, Russia

Tanmay Vachaspati²

Physics Department, Case Western Reserve University
Cleveland, OH 44106, USA.

Abstract

We describe certain aspects of ${}^3\text{He}$ and compare them to related aspects of the standard electroweak model of particle physics. We note various similarities in the order parameter structure, defect structure, interactions with fermions and anomalies in the two systems. Many issues in the condensed matter literature that are often confusing to the particle physics reader and vice versa are clarified.

¹volovik@boo.jum.hut.fi

²txv7@po.cwru.edu

Contents

| | | |
|----------|-----------------------------------------------------------------------------------------|-----------|
| 1 | Introduction | 3 |
| 2 | ^3He and the electroweak model: similarities | 4 |
| 2.1 | Broken symmetry | 4 |
| 2.2 | Bosonic sector of the Electroweak Model | 8 |
| 2.3 | Bosonic sector of ^3He | 9 |
| 3 | Strings | 12 |
| 3.1 | Singular Strings | 12 |
| 3.2 | Continuous Textures | 16 |
| 3.3 | Topology of Vortex Textures | 17 |
| 3.4 | Observation and Transition of Vortices | 19 |
| 4 | Fermions and gauge fields | 21 |
| 4.1 | Fermionic sector of the electroweak model | 21 |
| 4.2 | Fermions in ^3He | 22 |
| 4.3 | Bosonic sector of ^3He -A on Level 2 of analogy | 28 |
| 5 | Anomalies | 30 |
| 5.1 | Baryon number anomaly in the electroweak model | 30 |
| 5.2 | Mass current anomaly in ^3He -A | 31 |
| 5.3 | Momentum exchange between the moving continuous vortex and heat bath. | 33 |
| 6 | Fermions on vortices and strings | 35 |
| 6.1 | Symmetry generators | 35 |
| 6.2 | Fermion Zero Modes and Symmetry of the Vortex | 37 |
| 6.3 | Fermion Zero Modes in semiclassical approach | 40 |
| 6.4 | Spectral Flow in Vortices: Callan-Harvey mechanism of anomaly cancellation | 41 |
| 6.5 | Three reactive forces acting on a moving vortex | 44 |
| 6.6 | Aharonov-Bohm effect and analog of the spinning string | 46 |
| 6.7 | Angular momentum anomaly | 48 |
| 7 | Conclusions | 52 |

1 Introduction

It is well recognized that there are many similarities between condensed matter systems and particle physics stemming from the fact that both systems are described by field theory. Most of the common phenomena - an example of which is spontaneous symmetry breaking - are yet to be confirmed in the particle physics scenario while they are quite routinely observed by condensed matter physicists. Several phenomena occurring in condensed matter systems are expected to also occur in speculative particle physics schemes. These include the possibility of topological defects with their potential astrophysical and cosmological consequences.

Particle physics as we know it today is accurately described by the standard model. The model has been remarkably successful and would almost universally be accepted if (and when) the Higgs particle is found. At the same time, it should be noted that only the perturbative features of the model have been put to the test and it would be worthwhile to have a better understanding of the non-perturbative aspects of the theory. Such an understanding may be crucial, for example, for testing the hypothesis that the baryon number of the universe was produced (baryogenesis) during the electroweak phase transition in the early universe. The possibility of directly testing the non-perturbative aspects of the standard model seem remote at this time. In addition, some insight as to what to expect can help in such attempts when the time comes. To gain some intuition, we need to find a condensed matter system with some similarities to the standard electroweak model.

^3He is a well-studied condensed matter system and has an order parameter that has rich structure and yields several different phases. The A-phase is particularly complex and the transition of ^3He to the A-phase closely resembles the electroweak symmetry breaking. This and other similarities between the standard electroweak model and ^3He have been noticed by one of us in earlier work [1]. Here we shall extend this earlier work with clarifying remarks and also point out differences in the two systems. In particular, we discuss the vortices of ^3He which are similar to the Z -strings of the electroweak model [2, 3] and connect the baryon number contained in configurations of Z -strings [4, 5] with the mass current anomaly in $^3\text{He-A}$.

The superfluid ^3He is a unique system among the other condensed matter, because it has the maximum symmetry breaking, which can be compared

only with the vacuum in the elementary particle physics. This results in a variety of topological defects in ${}^3\text{He}$, such as monopoles, hedgehogs, boojums, solitons, domain walls, textures, quantized vortices, half-quantum vortices (the counterpart of the Alice strings), strings terminating on monopoles and domain walls terminating on strings, etc., and in related phenomena such as topological confinement, symmetry breaking with parity violation in the vortex core, Aharonov-Bohm effect on global strings, topological transitions, transitions mediated by monopoles and hedgehogs, bosonic and fermionic zero modes on vortices, genesis of the fermionic charges by moving vortices, vacuum polarization and vacuum instability. This makes the superfluid ${}^3\text{He}$ a working laboratory for modelling different processes which can occur in the physical vacuum.

2 ${}^3\text{He}$ and the electroweak model: similarities

There are two “levels” on which ${}^3\text{He}$ -A and the standard electroweak model resemble each other:

Level 1: The symmetry group of ${}^3\text{He}$ -A and of the standard electroweak model are very similar.

Level 2: The interactions of the low energy fermions with the ${}^3\text{He}$ -A order parameter closely resembles the interactions of the fermions in the electroweak model with the gauge fields present in the model.

2.1 Broken symmetry

The symmetry group G_{ew} of the standard electroweak model is:

$$G_{ew} = [SU(2)_T \times U(1)_Y]/Z_2 . \quad (2.1.1a)$$

Here $SU(2)_T$ is the group of isotopic rotations with the generator \mathbf{T} . The symmetry group $G_{3\text{He}}$ in liquid ${}^3\text{He}$

$$G_{3\text{He}} = SO(3)_S \times SO(3)_L \times U(1)_N , \quad (2.1.1b)$$

contains the groups of the independent *orbital* and *spin* rotations: the operator \mathbf{L} is the generator of the orbital rotations $SO(3)_L$, while the spin

operator \mathbf{S} is the generator of the spin rotations $SO(3)_S$. The operator \mathbf{N} of ${}^3\text{He}$ particle number plays the part of hypercharge \mathbf{Y} .

After the electroweak transition the little symmetry group H of the electroweak vacuum is

$$H_{\text{ew}} = U(1)_Q \equiv U(1)_{T_3+Y/2} , \quad (2.1.2a)$$

where $\mathbf{Q} = \mathbf{T}_3 + (1/2)\mathbf{Y}$ is the generator of electric charge.

After the superfluid transition of ${}^3\text{He}$ into the A-phase state the vacuum becomes anisotropic. The spin rotation $SO(3)_S$ symmetry group is reduced to its $SO(2)_S = U(1)_{S_3}$ subgroup; while the breaking of the other two symmetry groups in Eq.(2.1.1b) occurs in the same manner as in the electroweak transition:

$$SO(3)_L \times U(1)_N \rightarrow U(1)_Q \equiv U(1)_{L_3-N/2} . \quad (2.1.2b)$$

Here we have ignored a Z_2 factor that arises from the mixing of orbital and spin rotations. We shall discuss this factor in Sec. 3.

Further we refer to the corresponding generator of the A-phase symmetry, which is a generalized angular momentum operator $\mathbf{Q} = \mathbf{L}_3 - (1/2)\mathbf{N}$, as the “electric” charge. It should be emphasized that even though the scenario of the symmetry breaking in the two systems have common features, the symmetry of the electroweak model is fully gauged while that of ${}^3\text{He-A}$ is fully global³.

The Higgs field (order parameter) in the electroweak model is the spinor

$$\Phi_{\text{ew}} = \begin{pmatrix} \phi^+ \\ \phi \end{pmatrix} , \quad (2.1.3a)$$

which is normalized by: $\Phi_{\text{ew}}^\dagger \Phi_{\text{ew}} = \eta_{\text{ew}}^2/2$ in the vacuum where $\eta_{\text{ew}} \sim 250\text{GeV}$. The order parameter in superfluid ${}^3\text{He}$ is a 3×3 complex matrix $A_{\alpha i}$ corresponding to the representation ($S = 1$, $L = 1$) of the rotation groups. (The 9 complex elements of this 3×3 matrix transform by a phase factor when acted by elements of the $U(1)_N$ group.) Under the spin rotations the matrix transforms as a vector in its Greek index, while under the orbital

³The “semilocal” limit of the electroweak model has also been used in studying electroweak defects [6]. In this limit, the $U(1)_Y$ symmetry is gauged but the $SU(2)_T$ symmetry is taken to be global. This is similar to the model of the anisotropic superconductivity in which $(SO(3)_S \times U(1)_N)/Z_2 \rightarrow U(1)_{S_2-N/2}$ [7]. The electron liquid in superconductors is electrically charged superfluid, as a result the $U(1)_N$ symmetry is gauged, while the $SO(3)_S$ symmetry is global.

rotations it transforms as a vector in its Latin index. In the A-phase vacuum of the superfluid ${}^3\text{He}$, the order parameter can be factorized:

$$A_{\alpha i} = \Delta_0 d_\alpha \Psi_i . \quad (2.1.3b)$$

where, $\Delta_0 \sim 10^{-7}eV$ is the temperature dependent amplitude of the gap in the quasiparticle spectrum (see below). Here the spin part of the order parameter - the unit vector $\hat{\mathbf{d}}$ - denotes the axis of the spontaneous magnetic anisotropy of the ${}^3\text{He-A}$ vacuum. The ${}^3\text{He-A}$ counterpart of the electroweak Higgs field is the orbital part of the order parameter and is written as a complex vector

$$\vec{\Psi}_{3\text{He-A}} = \frac{\hat{e}_1 + i\hat{e}_2}{\sqrt{2}} , \quad (2.1.3c)$$

with $\hat{e}_1 \cdot \hat{e}_1 = \hat{e}_2 \cdot \hat{e}_2 = 1$, $\hat{e}_1 \cdot \hat{e}_2 = 0$.

The orbital anisotropy axis

$$\vec{l}_{3\text{He-A}} = i \frac{\vec{\Psi} \times \vec{\Psi}^\dagger}{\vec{\Psi}^\dagger \cdot \vec{\Psi}} = \hat{e}_1 \times \hat{e}_2 . \quad (2.1.4a)$$

gives the direction of the spontaneous orbital momentum $\langle \text{vac} | \mathbf{L} | \text{vac} \rangle$ in ${}^3\text{He-A}$. It plays the part of the spontaneous isotopic spin $\langle \text{vac} | \mathbf{T} | \text{vac} \rangle$ in the electroweak vacuum:

$$\vec{l}_{ew} = - \frac{\Phi^\dagger \vec{\tau} \Phi}{\Phi^\dagger \Phi} , \quad (2.1.4b)$$

where $\vec{\tau}$ are the Pauli matrices in the isotopic space. (For convenience we will drop the subscripts ew and ${}^3\text{He-A}$ on Ψ and $\vec{\Psi}$ in what follows.)

In ${}^3\text{He-A}$ the superfluid velocity of the vacuum flow is

$$\vec{v}_s = - \frac{i\hbar}{4m_3} \frac{(\Psi_i^\dagger \vec{\nabla} \Psi_i - \vec{\nabla} \Psi_i^\dagger \Psi_i)}{\vec{\Psi}^\dagger \cdot \vec{\Psi}} , \quad (2.1.5a)$$

where m_3 the mass of the ${}^3\text{He}$ atom. This velocity leads to the superfluid mass current in the ${}^3\text{He-A}$ vacuum (the mass current in the nonrelativistic condensed matter coincides with the density of the linear momentum):

$$\vec{j}_N = m_3 n_N \vec{v}_s , \quad (2.1.6)$$

where n_N is the particle density of the ${}^3\text{He-A}$ vacuum (the total N charge of the ${}^3\text{He-A}$ vacuum is the number of the ${}^3\text{He}$ atoms: $N = \int dV n_N$). In

excited state or at nonzero temperature T this current is supplemented by the current of thermal fermions:

$$\sum_{\vec{p}} \vec{p} f(\vec{p}) = \rho_n (\vec{v}_n - \vec{v}_s) , \quad (2.1.7)$$

where

$$f = (\exp[E_{\vec{p}} + \vec{v}_s \cdot \vec{p} - \vec{v}_n \cdot \vec{p}]/T + 1)^{-1}$$

is the Fermi function; $E_{\vec{p}}$ is the spectrum of the single-particle fermionic excitations; \vec{v}_n is the velocity of the heat bath (usually denoted as the velocity of the normal component of the liquid) and ρ_n is the density of the normal component (ρ_n is a tensor in anisotropic $^3\text{He-A}$). The total mass current of homogeneous superfluid is thus

$$\vec{j}_N = (m_3 n_N - \rho_n) \vec{v}_s + \rho_n \vec{v}_n = \rho_s \vec{v}_s + \rho_n \vec{v}_n , \quad (2.1.8a)$$

and the quantity $\rho_s = m_3 n_N - \rho_n$ is the so called (tensorial) density of the superfluid component of the liquid which appears below T_c as the manifestation of the breaking of $U(1)_N$ symmetry. Close to T_c one has $\rho_s \propto m_3 n_N (\Delta_0(T)/T_c)^2$ with $(\Delta_0(T)/T_c)^2 \sim 1 - T/T_c$.

In the electroweak vacuum the superfluid current corresponds to the hypercharge current of the vacuum which appears as a result of the breaking of $U(1)_Y$ symmetry

$$\vec{j}_Y = (\Phi^\dagger \Phi) \vec{v}_s , \quad (2.1.8b)$$

with $\Phi^\dagger \Phi \propto 1 - \frac{T}{T_c}$ near T_c . The corresponding ‘‘superfluid velocity’’ \vec{v}_s is expressed in terms of the spinor order parameter

$$\vec{v}_s = \frac{\Phi^\dagger \vec{D} \Phi - (\vec{D} \Phi)^\dagger \Phi}{2\Phi^\dagger \Phi} , \quad \vec{D} = -i\vec{\nabla} \mathbf{1} - \vec{\mathbf{W}} - \vec{\mathbf{Y}} . \quad (2.1.9)$$

where, $\vec{\mathbf{W}} = \tau_\alpha \vec{W}_\alpha/2$ and $\vec{\mathbf{Y}} = \mathbf{Y}/2$ are the $SU(2)_T$ and $U(1)_Y$ gauge fields. The difference between the electroweak model and $^3\text{He-A}$ is due to the gauge versus global symmetry groups of the two systems: The equation (2.1.9) for the electroweak current contains the gauge field $Z = T_3 - Y/2$.

In the electroweak case one can define 4 conserved currents corresponding to the 4 generators of the symmetry group $SU(2)_T \times U(1)_Y$. In the case of normal ^3He there are 7 generators of the symmetry group $SO(3)_S \times SO(3)_L \times U(1)_N$, but only 4 currents are conserved and have physical meaning. These

are: the mass current related to N (which corresponds to the hypercharge current) and 3 spin currents related to the $SO(3)_S$ generators. The “internal” orbital momentum \vec{L} of the Cooper pairs is not a conserved quantity, because it can be transferred to the “external” orbital momentum $\vec{r} \times \vec{j}_N$ associated with the macroscopic flow. That is why after the symmetry breaking into the $^3\text{He-A}$ state, on the **Level 1** there is no analog to the (conserved) current of the little group (electromagnetism). (Interaction between the internal and external orbital momenta is important for the vortex structure in $^3\text{He-A}$ (see Eq.(3.1.8)).

When the orbital anisotropy axis, $\hat{\mathbf{l}}$, is constant, the superfluid velocity \vec{v}_s is the gradient of the phase of the order parameter and thus is curl-free. If, however, $\hat{\mathbf{l}}$ varies in space, forming the so-called $\hat{\mathbf{l}}$ -texture, the $^3\text{He-A}$ mass flow acquires vorticity, which is expressed in terms of the $\hat{\mathbf{l}}$ field by the Mermin-Ho relation [8]:

$$\vec{\nabla} \times \vec{v}_s = \frac{\hbar}{4m_3} e_{ijk} \hat{l}_i \vec{\nabla} \hat{l}_j \times \vec{\nabla} \hat{l}_k . \quad (2.1.10)$$

This follows from Eq.(2.1.5a).

2.2 Bosonic sector of the Electroweak Model

The standard model of the electroweak interactions is an $SU(2) \times U(1)$ invariant theory with a scalar field Φ in the fundamental representation of $SU(2)$. The bosonic sector of the model is described by the Lagrangian:

$$L_b = L_W + L_Y + L_\Phi - V(\Phi_{\text{ew}}) \quad (2.2.1)$$

where,

$$L_W = -\frac{1}{4g^2} W_{\mu\nu a} W^{\mu\nu a} \quad (2.2.2)$$

$$L_Y = -\frac{1}{4g'^2} Y_{\mu\nu} Y^{\mu\nu} \quad (2.2.3)$$

where $W_{\mu\nu}^a$ and $Y_{\mu\nu}$ are the field strengths for the $SU(2)_T$ and $U(1)_Y$ gauge fields W_μ^a and Y_μ respectively. Also,

$$L_\Phi = |D_\lambda \Phi_{\text{ew}}|^2 \equiv \left| \left(\partial_\lambda - \frac{i}{2} \tau^a W_\lambda^a - \frac{i}{2} Y_\lambda \right) \Phi_{\text{ew}} \right|^2 \quad (2.2.4)$$

$$V(\Phi_{ew}) = \lambda(\Phi_{ew}^\dagger \Phi_{ew} - \eta_{ew}^2/2)^2, \quad (2.2.5)$$

where,

$$\Phi_{ew} = \begin{pmatrix} \phi^+ \\ \phi \end{pmatrix}, \quad (2.1.3a)$$

is a complex doublet.

Below the symmetry breaking transition the transverse fields W_μ^1 , W_μ^2 and the following combination of the longitudinal W_μ^3 field and Y_μ

$$Z_\mu \equiv l_{ew}^a W_\mu^a - Y_\mu \quad (2.2.6)$$

acquire masses, while the combination

$$A_\mu \equiv \sin^2 \theta_W l_{ew}^a W_\mu^a + \cos^2 \theta_W Y_\mu, \quad (2.2.7)$$

remains massless. This massless gauge field represents the little group $U(1)_Q$ of electromagnetism. Here \hat{l}_{ew} is the unit vector defined in Eq. (2.1.4b); the weak mixing angle θ_W and electric charge e are given by the equations $e = g \sin \theta_W = g' \cos \theta_W$.

2.3 Bosonic sector of ^3He

In superfluid ^3He the bosonic sector consists of two groups: (i) The soft variables, which are the densities of the conserved quantities. They exist even in normal state above transition. These are the particle density n_N , the spin density \vec{S} and the density of the linear momentum \vec{j}_N . The latter is usually expressed in terms of the velocity of the liquid: in the normal liquid above transition $\vec{j}_N = m_3 n_N \vec{v}$; in superfluid state this variable transforms to the normal velocity \vec{v}_n of the heat bath of fermionic (and/or bosonic) excitations in Eq.(2.1.8a). (ii) The order parameter (Higgs) field $A_{\alpha i}$ which appears below transition. In general the dynamics of all these variables is not described by a Lagrangian because of dissipation and the nontrivial interaction of these variables with the fermionic degrees of freedom. There are only a few regimes where a simple Lagrangian description is possible: (1) Close to T_c there is the Ginzburg-Landau free energy functional, which describes the static Higgs fields $A_{\alpha i}$. In some cases the Ginzburg-Landau description can be extended to include the time dependence.

(2) Hydrodynamic description in terms of only the soft variables ($n_N, \vec{S}, \vec{v}_n +$ Goldstone bosons sector of the Higgs fields) works in all temperature regimes if the dynamics is slow enough as compared to the time of establishment of the local thermal equilibrium.

(3) The quantum field theory at near zero temperature, where the dynamics of the soft bosons and low energy fermions can be constructed.

We will now discuss each of these descriptions in some detail.

The *Ginzburg-Landau free-energy functional* must be invariant under the total symmetry group G of the physical laws. This invariance essentially restricts the number of fourth-order terms and also the number of gradient terms that can be written. In superfluid ^3He it contains one second-order term, five fourth-order terms and three gradient terms. In each of them the Greek spin indices should not be mixed with the Latin orbital indices to provide the invariance under separate spin $SO(3)_{(S)}$ and orbital $SO(3)_{(L)}$ rotations; also each term should contain an equal number of $A_{\alpha i}^*$ and $A_{\alpha i}$ for invariance under $U(1)_N$ transformations. As a result of these requirements $F^{G-L}[A_{\alpha i}]$ is given by [9]

$$\begin{aligned}
F^{G-L} = & -\alpha A_{\alpha i}^* A_{\alpha i} + \beta_1 A_{\alpha i}^* A_{\alpha i}^* A_{\beta j} A_{\beta j} + \beta_2 A_{\alpha i}^* A_{\alpha i} A_{\beta j}^* A_{\beta j} + \beta_3 A_{\alpha i}^* A_{\beta i}^* A_{\alpha j} A_{\beta j} \\
& + \beta_4 A_{\alpha i}^* A_{\beta i} A_{\beta j}^* A_{\alpha j} + \beta_5 A_{\alpha i}^* A_{\beta i} A_{\beta j} A_{\alpha j}^* \\
& + \gamma_1 D_j^* A_{\alpha i}^* D_j A_{\alpha i} + \gamma_2 D_j^* A_{\alpha i}^* D_i A_{\alpha j} + \gamma_3 D_j^* A_{\alpha j}^* D_i A_{\alpha i} .
\end{aligned} \tag{2.3.1}$$

Here $\vec{D} = -i\vec{\nabla} - m_3\vec{v}_n$, where the velocity of the normal component is fixed; the parameter α changes sign at T_c , $\alpha = \alpha_0(1 - T/T_c)$, while α_0 and the β 's are functions of pressure only and depend on the details of the microscopic interaction of the ^3He atoms. Note that the last two gradient terms are not invariant under separate (isotopic) orbital rotation of the order parameter: this results from the interaction of the internal and external orbital rotations.

The vacuum manifold resulting from the minimization of the Ginzburg-Landau functional depends on the parameter values entering eq. (2.3.1) and hence on the temperature and pressure. Therefore, the values of the temperature and pressure determine the superfluid phase.

The Ginzburg-Landau functional is also useful for determining the core structure of singular topological defects, within which the order parameter deviates from its vacuum values. The core size is of the order of coherence length

$$\xi(T) \sim \sqrt{\gamma/\alpha} \sim (200 - 500)(1 - T/T_c)^{-1/2} A^o .$$

This corresponds to the scale $\xi(T) = 1/m_{Higgs}(T)$ determined by the inverse mass of the Higgs boson in electroweak theory, which defines the core size of Z string.

The *hydrodynamic or London energy* is the energy of fields on the vacuum manifold of a given superfluid phase. In $^3\text{He-A}$ the London energy is given in terms of the mass density $\rho = m_3 n_N$, spin density \vec{S} , velocity \vec{v}_n of the normal component, orbital Goldstone variables $\vec{v}_s, \hat{\mathbf{l}}$ and spin Goldstone field $\hat{\mathbf{d}}$:

$$\begin{aligned}
F^{London} = & F(\rho, T) + \frac{1}{2}\gamma^2 S_\alpha (\chi^{-1})_{\alpha\beta} S_\beta - \gamma \vec{B} \cdot \vec{S} + \frac{1}{2}(\rho\delta_{ij} - (\rho_s)_{ij})(\vec{v}_n)_i(\vec{v}_n)_j \\
& + \frac{1}{2}(\rho_s)_{ij}(\vec{v}_s)_i(\vec{v}_s)_j + \frac{1}{2}K_{ijmn}\partial_i\hat{\mathbf{l}}_m\partial_j\hat{\mathbf{l}}_n + C_{ij}(\vec{v}_s)_i(\vec{\nabla} \times \hat{\mathbf{l}})_j \\
& + \frac{1}{2}(\rho_{sp})_{ij}\nabla_i\hat{\mathbf{d}}_\alpha\nabla_j\hat{\mathbf{d}}_\alpha - \frac{1}{2}g_{so}(\hat{\mathbf{d}} \cdot \hat{\mathbf{l}})^2 . \tag{2.3.2}
\end{aligned}$$

Here \vec{v}_s is defined with the factor $\hbar/2m_3$ multiplied into Eq.(2.1.5a); the tensors $(\rho_s)_{ij}$, C_{ij} , $(\rho_{sp})_{ij}$ and K_{ijmn} are uniaxial tensors with the anisotropy axis along $\hat{\mathbf{l}}$:

$$(\rho_s)_{ij} = \rho_s^\parallel \hat{\mathbf{l}}_i \hat{\mathbf{l}}_j + \rho_s^\perp (\delta_{ij} - \hat{\mathbf{l}}_i \hat{\mathbf{l}}_j) , \tag{2.3.3}$$

$$C_{ij} = C\delta_{ij} - C_0 \hat{\mathbf{l}}_i \hat{\mathbf{l}}_j , \tag{2.3.4}$$

$$\frac{1}{2}K_{ijmn}\partial_i\hat{\mathbf{l}}_m\partial_j\hat{\mathbf{l}}_n = \frac{1}{2}\left[K_1(\vec{\nabla} \cdot \hat{\mathbf{l}})^2 + K_2(\hat{\mathbf{l}} \cdot (\vec{\nabla} \times \hat{\mathbf{l}}))^2 + K_3(\hat{\mathbf{l}} \times (\vec{\nabla} \times \hat{\mathbf{l}}))^2\right] . \tag{2.3.5}$$

Here K_1 , K_2 , and K_3 are the twist, splay, and bend coefficients respectively, and, $\chi_{\alpha\beta}$ is a uniaxial tensor with the anisotropy axis along $\hat{\mathbf{d}}$:

$$\chi_{\alpha\beta} = \chi_\parallel \hat{\mathbf{d}}_\alpha \hat{\mathbf{d}}_\beta + \chi_\perp (\delta_{\alpha\beta} - \hat{\mathbf{d}}_\alpha \hat{\mathbf{d}}_\beta) . \tag{2.3.6}$$

\vec{B} is an external magnetic field interacting with the spin density. The last term in Eq.(2.3.2) describes the tiny spin-orbital coupling between $\hat{\mathbf{d}}$ and $\hat{\mathbf{l}}$.

This functional is useful for determination of the continuous structures of the Goldstone fields (textures) in which the system does not leave the vacuum manifold.

The mass current in the London limit is

$$m_3(\vec{j}_N)_i = \frac{\partial F^{London}}{\partial v_{si}} + \frac{\partial F^{London}}{\partial v_{ni}}$$

$$= (\rho_s)_{ij}(\vec{v}_s)_j + (\rho\delta_{ij} - (\rho_s)_{ij})(\vec{v}_n)_j + C_{ij}(\vec{\nabla} \times \hat{\mathbf{1}})_j . \quad (2.3.7)$$

The current contains three terms of which the first and second are due to the superfluid and normal component motion and the third is due to the $\hat{\mathbf{1}}$ texture.

The *quantum description* includes the dynamics of Goldstone fields and the propagation of the elementary particles (fermions and bosons) in the potentials produced by these Goldstone fields. Typical example is the interaction of the fermionic particle with the field of quantized vortex.

3 Strings

3.1 Singular Strings

The **Level 1** analogy between the electroweak model and ${}^3\text{He}$ leads to similarity in the structure of defects in the two models, though there are important differences too. The main difference is that the topology of the vacuum manifold in the electroweak model does not support topologically stable strings while the vacuum manifold for ${}^3\text{He-A}$ admits topological strings in addition to analogs of electroweak strings. The fundamental homotopy group of the electroweak vacuum manifold

$$M_{\text{ew}} = G_{\text{ew}}/H_{\text{ew}} = SU(2) \quad (3.1.1)$$

is trivial: $\pi_1(M_{\text{ew}}) = 0$.

In contrast, the A-phase manifold

$$M_{\text{A}} = G_{{}^3\text{He}}/H_{\text{A}} = (SO(3) \times S^2)/Z_2 \quad (3.1.2)$$

has nontrivial fundamental group

$$\pi_1(M_{\text{A}}) = Z_4 , \quad (3.1.3)$$

which contains four elements. There are two reasons for this: (i) instead of $SU(2)$ in M_{ew} the A-phase manifold M_{A} contains the group $SO(3) = SU(2)/Z_2$, and, (ii) the full symmetry group of the A-phase vacuum:

$$H_{\text{A}} = U(1)_{S_3} \times U(1)_{L_3-N/2} \times Z_2 . \quad (3.1.4)$$

contains another Z_2 factor. This is the symmetry under rotation of the spin axis, $\hat{\mathbf{d}}$, by π about an axis perpendicular to $\hat{\mathbf{d}}$ followed by a rotation of the triad $(\hat{e}_1, \hat{e}_2, \hat{\mathbf{I}})$ by π about $\hat{\mathbf{I}}$ in orbital space. According to Eq.(2.1.3b), this leaves the full order parameter invariant. Both discrete symmetries Z_2 , being combined, give the Z_4 in Eq.(3.1.3).

This means that there are 4 topologically distinct classes of strings in $^3\text{He-A}$. Each can be described by the topological charge ν which takes only 4 values, which we choose to be $0, \pm 1/2$ and 1 with summation modulo 2 (ie. $1+1=0$).

Let us now construct different strings and distribute them into classes characterized by the charge ν . The strings - corresponding to $U(1)$ vortices with integer winding number n - have the following asymptotic form:

$$A_{\alpha j}(r \rightarrow \infty, \phi) = \Delta_0 e^{in\phi} \hat{z}_\alpha(\hat{x}_j + i\hat{y}_j) \quad . \quad (3.1.5a)$$

The circulation of the superfluid velocity around the vortex core is quantized

$$\oint d\vec{r} \cdot \vec{v}_s = \kappa n \quad , \quad \kappa = \frac{2\pi\hbar}{2m_3} \quad , \quad (3.1.6)$$

and κ is called the circulation quantum. The order parameter phase ϕ is not defined on the vortex axis, i.e. the vorticity is singular on the vortex axis.

The asymptotic form of vortices with fractional circulation number $n = \pm 1/2$ (or, simply, half-quantum vortices) is given by

$$A_{\alpha j}(r \rightarrow \infty, \phi) = \Delta_0 e^{\pm i\phi/2} (\hat{x}_\alpha \cos \frac{\phi}{2} + \hat{y}_\alpha \sin \frac{\phi}{2})(\hat{x}_j + i\hat{y}_j) \quad . \quad (3.1.5b)$$

On circumnavigating such a vortex, the change of the sign of the order parameter due to the phase winding by π , is compensated by the change of sign of the vector $\vec{\mathbf{d}} = \hat{\mathbf{x}} \cos \frac{\phi}{2} + \hat{\mathbf{y}} \sin \frac{\phi}{2}$. This vortex is the counterpart of Alice strings considered in particle physics[10]: a particle that goes around an Alice string flips its charge. In $^3\text{He-A}$ the quasiparticle going around a $1/2$ vortex flips its $U(1)_{S_3}$ charge, that is, its spin. As a consequence, several phenomenon (*eg.* global Aharanov-Bohm effect) discussed in the particle physics literature have corresponding discussions in the condensed matter literature (see [11],[12] for $^3\text{He-A}$ and [13] in particle physics). Note that in $^3\text{He-A}$ also the particle-like topological object, the hedgehog, flips its π_2 topological charge around the $1/2$ vortex [14] .

All the vortices in ${}^3\text{He-A}$ can now be grouped in accordance with their π_1 topological charge ν . The half-quantum vortices belong to the classes $\nu = \pm 1/2$; the vortices with odd circulation number, $n = 2k + 1$, belong to the class $\nu = 1$, and the vortices with even circulation number, $n = 2k$, have zero topological charge $\nu = 0$. The latter means that, as distinct from lines with $\nu = \pm 1/2, 1$, the singularity in these $\nu = 0$ strings, such as $n = 2$ vortex, can be continuously dissolved. What is left is called “texture” with continuously distributed (non-singular) order parameter within the vacuum manifold.

The $n = 2$ ($\nu = 0$) topologically unstable vortex corresponds to the unit winding Z string in the electroweak model. Both the Z -string and the ${}^3\text{He-A}$ $n = 2$ vortex have constant $\vec{l} = \hat{z}$, and, in both cases the phase of the order parameter has a singularity at $r = 0$. The Higgs field configuration for a Z -string is:

$$\Phi_{Z\text{-string}}(\vec{r}) = \frac{\eta}{\sqrt{2}} f(r) e^{i\phi} \begin{pmatrix} 0 \\ 1 \end{pmatrix} , \quad (3.1.7)$$

in cylindrical coordinates. In the electroweak case, the form of the Higgs field alone does not describe a string and the gauge fields must also be specified. The only non-vanishing gauge field in the Z -string is $Z_\phi = -2v(r)/(\alpha r)$ where $v(0) = 0$ and $v(\infty) = 1$. Like in superconductors, due to Meissner effect the gauge field Z screens the superfluid velocity far from the core, where $\oint d\vec{r} \cdot \vec{v}_s \rightarrow 0$. This is different from the electrically neutral ${}^3\text{He}$ where this complication is absent since there are no gauge fields and circulation is conserved quantity (if $\hat{l} = \hat{z}$ is fixed).

The singularity at the origin is smoothed out by escaping the Higgs field from its vacuum manifold with $f = 1$. In the axisymmetric Z -string one has $f(0) = 0$ and $f(r \gg \xi(T)) = 1$ at radial infinity (Fig.1a). In ${}^3\text{He-A}$ the behavior within the core of the size $\sim \xi(T)$ is slightly different. The structure of the axially symmetric Higgs field in the A-phase vortex core is described by two radial functions consistent with the axial symmetry (Fig.1b):

$$A_{\alpha j}(r, \phi) = \Delta_0 \hat{z}_\alpha [e^{in\phi} f_1(r)(\hat{x}_j + i\hat{y}_j) + e^{i(n+2)\phi} f_2(r)(\hat{x}_j - i\hat{y}_j)] . \quad (3.1.5c)$$

Here $f_1(r \gg \xi(T)) = 1$, $f_2(r \gg \xi(T)) = 0$, $f_1(0) = 0$, while $f_2(0)$ depends on n : at $n = -2$ the parameter $f_2(0)$ is finite, i.e. the Higgs field does not necessarily disappear in the vortex core.

The reason for the appearance of the $f_2(r)$ term as compared with the electroweak string is the interaction of the internal (isotopic) orbital rotations

$SO(3)_L$ of the vectors \hat{e}_1 and \hat{e}_2 with the coordinate rotations. The order parameter in Eq. (3.1.5c) is the eigenstate of the total angular momentum $\mathbf{L}_3^{\text{total}}$

$$\mathbf{L}_3^{\text{total}} = \mathbf{L}_3^{\text{int}} + \frac{1}{i}\partial_\phi \ , \quad (3.1.8)$$

with $L_3^{\text{total}} = n + 1$. This momentum is distributed between the internal and external momenta in the following way: in the first term $L_3^{\text{int}} = 1$, $L_3^{\text{ext}} = n$, while in the second one $L_3^{\text{int}} = -1$, $L_3^{\text{ext}} = n + 2$. The second term represents the component of the Higgs field with the opposite orientation of the $\hat{\mathbf{l}}$, which appears in the vortex core. (Also see Sec.(6.1).) In the electroweak string such component can appear only by the additional spontaneous symmetry breaking in the vortex core due to the instability of Z-string induced, say, by the fermion zero modes [15].

The $n = 2$ singular line in ${}^3\text{He-A}$ and Z -string are topologically unstable, since even with given asymptote at $r \rightarrow \infty$ the singular core where the Higgs field deviates from its vacuum value can be removed by the formation of the continuous $\hat{\mathbf{l}}$ texture with the vacuum manifold everywhere in space (Anderson-Toulouse-Chechetkin vortex,[16], see Sec.3.2). That is, in ${}^3\text{He-A}$ [17] and in the electroweak model, the vortices can terminate on a $\hat{\mathbf{l}}$ hedgehog ($\hat{\mathbf{l}} = \hat{r}$); in particle physics this hedgehog configuration is a *magnetic monopole* of the 't Hooft-Polyakov type with an additional physical string [2].

In the electroweak model, we also have the W -string solutions. They correspond to the so called disgyrations in ${}^3\text{He-A}$: the lines with winding of the $\hat{\mathbf{l}}$ -vector without winding of the phase. For example two (gauge equivalent) W -string configurations are:

$$\Phi^{(1)}(r, \phi) = \frac{\eta}{\sqrt{2}}f_W(r) \begin{pmatrix} \cos \phi \\ i \sin \phi \end{pmatrix} \ ,$$

$$\mathbf{W}^1 = \frac{v_W(r)}{r}\hat{e}_\phi \ , \quad \mathbf{W}^2 = \mathbf{W}^3 = \mathbf{B} = 0 \quad (3.1.9)$$

$$\Phi^{(2)}(r, \phi) = \frac{\eta}{2}f_W(r) \begin{pmatrix} e^{i\phi} \\ e^{-i\phi} \end{pmatrix} \ ,$$

$$\mathbf{B} = \mathbf{W}^1 = \mathbf{W}^2 = 0, \quad \mathbf{W}^3 = \frac{v_W(r)}{r}\hat{e}_\phi, \quad (3.1.10)$$

where, the subscript W on the profile functions f and v means that the functions are the ones appropriate to the W -string. In ${}^3\text{He}$, the W -strings correspond to the topologically unstable disgyrations with $n_l = 2$ winding number for the $\hat{\mathbf{l}}$ -vector around the line:

$$\hat{\mathbf{l}}^{(1)} = \hat{z} \cos 2\phi + \hat{y} \sin 2\phi \quad , \quad \hat{\mathbf{l}}^{(2)} = \hat{x} \cos 2\phi - \hat{y} \sin 2\phi \quad . \quad (3.1.11)$$

Thus we see that the similar symmetry groups of ${}^3\text{He}$ and the electroweak model lead to similar vortex and monopole structures in the two systems. The different nature of the symmetries - global versus gauge - does not play a role in the topology of such textures in the two systems, though it does influence the energetics of these defects.

3.2 Continuous Textures

In ${}^3\text{He-A}$, the “textures” - spatially inhomogenous distributions in the vector fields $\hat{\mathbf{d}}$ and $\hat{\mathbf{l}}$ - are similar to those in liquid crystals and in ferro- and antiferromagnets. (Note that in cosmology a texture has a more narrow meaning: it is a point-like object - Skyrmion - with a continuous distribution of the order parameter described by the topological charge of the homotopy group $\pi_3(M)$). The spatial scales of these textures are defined either by the dimension of the vessel or by some fine interaction like tiny spin-orbit coupling $-(1/2)g_{so}(\hat{\mathbf{d}} \cdot \vec{l})^2$ in Eq.(2.3.2) and interaction $\hat{\mathbf{d}}$ with external magnetic field. These scales are essentially larger than the coherence length $\xi(T)$ which defines the core of singular defects.

A domain wall in soft ferromagnets is one of the numerous examples of textures which scale essentially exceeds $\xi(T)$. This texture exists due to small spin-orbit coupling of magnetization \vec{S} with the crystallographic direction of the easy axis $-(1/2)g_{so}(\hat{z} \cdot \vec{S})^2$. This interaction reduces the $M = S^2$ vacuum manifold of the isotropic ferromagnet to the manifold $\tilde{M} = Z_2$, which contains 2 disconnected pieces $\vec{S} = \pm S\hat{z}$. Stability of the domain wall is guaranteed by the nontrivial group $\pi_0(\tilde{M}) = Z_2$: the domain wall in ferromagnets can be either closed or terminate on the boundary of the system but it cannot have a boundary.

In ${}^3\text{He-A}$ the situation is more complicated: the vacuum manifold M_A contains only one connected piece, even when it is reduced by the spin-orbit interaction. In the presence of the spin-orbit coupling the reduced

vacuum manifold is $\tilde{M}_A = \tilde{G}/\tilde{H}_A$. Here the initial symmetry group $\tilde{G} = SO(3)^J \times U(1)$ contains only simultaneous spin and orbital rotations and the invariant subgroup is $\tilde{H}_A = SO(2)^J \times U(1)$. As a result $\pi_0(\tilde{M}_A)$ is trivial, and does not support topological domain walls. Nevertheless, one can construct a continuous planar texture, separating two volumes with different orientation of $\hat{\mathbf{l}}$ with respect to $\hat{\mathbf{d}}$ (see Fig. 2). This looks like a domain wall in ferromagnets, but the topology which supports its stability is different. This wall can terminate and the edge of the wall is the location of a topologically stable singular line: a 1/2-quantum vortex. Therefore this wall cannot be destroyed in a non-singular way - that is, the order parameter must leave the vacuum manifold M_A if the wall is to terminate - and thus it also has a topological charge. As distinct from walls with nontrivial π_0 we call this object a topological *soliton*. Such solitons were identified in NMR experiments on $^3\text{He-A}$. (See Reference [18] where the crossing of the soliton with the nonsingular Anderson-Toulouse-Chechetkin vortices has been observed. The crossing point represents the “texture” in the particle physics sense: like a Skyrmion it is described by the π_3 topology [19]).

The stability of the soliton is dictated by the same homotopy group, which is responsible for the stability of walls bounded by strings, discussed in cosmology [20]. This is the relative homotopy group $\pi_1(M_A, \tilde{M}_A)$, which deals with different vacuum manifolds at different scales: far from the soliton at a distance larger than the characteristic length ξ_D of spin-orbit coupling the vectors $\hat{\mathbf{d}}$ and $\hat{\mathbf{l}}$ are locked together (we call this as a dipole locking) and the vacuum manifold is reduced to \tilde{M}_A , while within the soft core of the soliton of size ξ_D it is again restored to M_A .

3.3 Topology of Vortex Textures

The axisymmetric $\hat{\mathbf{l}}$ texture is defined by two radially dependent functions:

$$\hat{\mathbf{l}} = \hat{z} \cos \eta(r) + \sin \eta(r)(\hat{r} \cos \alpha(r) + \hat{\phi} \sin \alpha(r)) \quad . \quad (3.3.1)$$

This is a general solution of the equation of the axisymmetry for the orbital texture:

$$\mathbf{L}_3^{\text{total}} \hat{\mathbf{l}}(\vec{r}) = 0 \quad , \quad (3.3.2)$$

where $\mathbf{L}_3^{\text{total}}$ is the generator of orbital rotations in eqn.(3.1.8).

The singular $n = 2$ vortex (and also the electroweak Z -string) corresponds to $\eta(r) = 0$ for all r . But there is another vortex - called the Anderson-Toulouse-Chechetkin 4π vortex - which is non-singular and which can be obtained by continuous deformations of the $n = 2$ vortex. This corresponds to having $\eta(r = 0) = 0$ and $\eta(r \geq r_0) = \pi$. The winding number of this vortex outside the core is:

$$n = \frac{1}{\kappa} \oint_{r>r_0} d\vec{r} \cdot \vec{v}_s = \frac{1}{\kappa} \int d\vec{S} \cdot \vec{\nabla} \times \vec{v}_s = \frac{1}{2\pi} \int dx dy \hat{\mathbf{l}} \cdot (\partial_x \hat{\mathbf{l}} \times \partial_y \hat{\mathbf{l}}) = 2 \quad , \quad (3.3.3)$$

Here we used the Mermin-Ho relation and the expression for the topological invariant which describes the mapping $S^2 \rightarrow S^2$ of the vortex cross-section to the sphere S^2 of the unit vector $\hat{\mathbf{l}} \cdot \hat{\mathbf{l}} = 1$. The invariant shows that within the continuous 4π -vortex the full area (4π) of the sphere is swept once.

The vortex core radius r_0 usually essentially exceeds $\xi(T)$: it can be limited by the next scale in the hierarchy of interactions, which can be the radius of the vessel or the scale ξ_D of the spin-orbit coupling. We call this the soft core compared to the hard core of the singular defect.

Thus the $n = 2$ vortex escaped the singularity but immediate pay for it is the broken parity: in the texture formed one has $\hat{\mathbf{l}}(\vec{r}) \neq \hat{\mathbf{l}}(-\vec{r})$, though some combined parity is still retained. This is one of the numerous examples in ${}^3\text{He}$, when the reduction of energy is accompanied by parity violation.

Such continuous vortices are described by π_2 homotopy. If $\hat{\mathbf{l}}$ is fixed at infinity we can define two charges of the vortex

$$\nu_l = \frac{1}{4\pi} \int dx dy \hat{\mathbf{l}} \cdot (\partial_x \hat{\mathbf{l}} \times \partial_y \hat{\mathbf{l}}) \quad , \quad (3.3.3)$$

and

$$\nu_d = \frac{1}{4\pi} \int dx dy \hat{\mathbf{d}} \cdot (\partial_x \hat{\mathbf{d}} \times \partial_y \hat{\mathbf{d}}) \quad , \quad (3.3.4)$$

These charges characterize the orientational distribution of the unit vectors $\hat{\mathbf{l}}$ and $\hat{\mathbf{d}}$. For the Anderson-Toulouse-Chechetkin vortex $\nu_l = n/2 = 1$, while ν_d can be either 1 or 0, depending on the (experimental) external conditions (see [21] and Fig.3).

In the particle physics literature, Preskill's semilocal skyrmion is analogous to the Anderson-Toulouse-Chechetkin vortex. In [22] the continuous deformation of a semilocal string (a Z -string in the limit that $SU(2)_T$ is global [6]) into a non-singular configuration is described. The final configuration is called a semilocal Skyrmion and corresponds directly to the global

Anderson-Toulouse-Chechetkin vortex in ${}^3\text{He-A}$. The semilocal Anderson-Toulouse-Chechetkin vortices in one of the models of the anisotropic superconductivity was considered in [7].

For a periodic vortex array in a rotating vessel these topological charges characterize the fields within an elementary cell of the vortex lattice. The vortex cell with $n = 2$ and $n = 4$ circulations along the cell boundary are most probable; Fig. 3b shows an elementary cell of the periodic texture with $n = 4$ circulation along the cell boundary. The situation for the $\hat{\mathbf{d}}$ texture is more diverse. Without magnetic field $\hat{\mathbf{d}}$ is dipole-locked with $\hat{\mathbf{l}}$, which means that the $\hat{\mathbf{d}}$ texture has the same π_2 charge as the $\hat{\mathbf{l}}$ texture and so: $\nu_d = 1$ for the texture in Fig. 3a and $\nu_d = 2$ for the texture in Fig. 3b.

The situation changes in an external magnetic field, where a new length scale appears. If we subject the texture to an axially oriented external magnetic field and start increasing its strength, the coupling of the magnetic part of the order parameter ($\hat{\mathbf{d}}$) to the field soon wins over the spin-orbit interaction and $\hat{\mathbf{d}}$ will become confined to the plane transverse to the magnetic field. The topology of the orbital $\hat{\mathbf{l}}$ field, which is responsible for the continuous vorticity, is insensitive to this process and thus $\nu_l = 1$, independently of the value of the field. However, the magnetic topological number ν_d will undergo a discontinuous change from 1 to 0. The final configuration is known as the “dipole-unlocked vortex”. In the center of a dipole-unlocked vortex a continuous (non-singular) “*soft*” *vortex core* with a diameter on the order of ξ_D is formed in which $\hat{\mathbf{d}}$ is dipole-unlocked from $\hat{\mathbf{l}}$. The change in the configuration of the $\hat{\mathbf{d}}$ texture as a function of magnetic field corresponds to a first order textural phase transition in the vortex structure (see below).

3.4 Observation and Transition of Vortices

Until now three types of quantized vortex lines [21] and the vortex sheet (the soliton with accumulated vorticity [23], see Fig. 3c) have been experimentally verified to exist in ${}^3\text{He-A}$ which is placed in a rotating container with an axial, external magnetic field (Fig. 4 and Ref.[21]). The three vortices are: 1) The dipole-locked continuous vortex, which have the following set of topological charges $\nu = 0$, $\nu_l = n/2 = 1$, $\nu_d = 1$ (Fig. 3a). 2) The dipole-unlocked continuous vortex with $\nu = 0$, $\nu_l = n/2 = 1$, $\nu_d = 0$ (Fig. 3a). 3) The singly quantized ($n = 1$) isolated vortex, which is singular since it has a nonzero π_1 charge ($\nu = 1$).

The structure of the latter vortex in Fig. 5 is rather peculiar: it has a hard (singular) core of size $\sim \xi(T)$, but in the vicinity of the core it represents not the vortex but the disgyration – the singular line in the $\hat{\mathbf{I}}$ field. It is analogous to the W -string in eqn.(3.1.11) but with unit winding number $n_l = 1$. This singular line has no singularity in the vorticity: the vorticity is thus continuous and is concentrated in a soft core of dimension ξ_D , in which the $\hat{\mathbf{I}}$ texture has the fractional π_2 charge $\nu_l = 1/2$, corresponding to the continuous vorticity of $n = 1$ vortex. Within the soft core the $\hat{\mathbf{I}}$ texture is dipole unlocked from the $\hat{\mathbf{d}}$ texture, which has $\nu_d = 0$. This dipole unlocked structure allows the observation of the $n = 1$ vortex in NMR experiments [21].

In the phase plane formed by the experimentally controlled variables Ω (angular velocity) and H (magnetic field strength) each of the three vortex arrays occupies a region where its energy is less than those of the others (Fig. 4a). These regions are separated from each other by first order phase transitions. This does not necessarily mean that in a given region of the $\Omega - H$ phase diagram we will always observe the equilibrium (least energy) vortex array. Since the transitions are of first order, a large energy barrier may separate two different vortex structures. A vortex may thus remain quite comfortably in a metastable state, even if the external variables are changed while it already exists and it is transported into a foreign territory of the phase diagram, where it is not the equilibrium structure. For example, the vortex sheet state of the rotating ${}^3\text{He}$ has been observed only as a metastable state. The region where the vortex sheet state has the lowest energy in the rotating container nevertheless exists (see Ref.[21] and Fig. 4b) but at higher rotation velocity.

Especially large energy barrier exists for the transition between the singular and continuous vortices. This process is possible from the topological point of view: the arithmetic summation laws for the charges n and ν ($1 + 1 = 2$ and $1 + 1 = 0$ correspondingly) show that the result from a fusion of two singular vortices is one continuous vortex. However such a process has not been observed because of the strong “Coloumb” repulsion of two global $n = 1$ vortices. This allows us to construct arbitrary mixtures of doubly and singly quantized vortices and to investigate the processes of phase separation in this two-component Coloumb plasma [24].

As distinct from the singular to continuous or continuous to singular transformations, which was never realized, the transformation of the dipole-

locked continuous to its dipole-unlocked modification has been recorded [25]. According to our current understanding the transition between two continuous vortices is mediated by a point-like object - a hedgehog or monopole in the $\hat{\mathbf{d}}$ -field - which represents the interface between two topologically different pieces of the vortex line (Fig. 6). Since the vortices on either side of their interface have different π_2 topological charges, $\nu_d = 0$ and $\nu_d = 1$, the interface between them is the $\hat{\mathbf{d}}$ hedgehog, which is described by the non-trivial element $\nu_d = 1$ of the homotopy $\pi_2(M_A) = Z$. This combination of a linear and a point defect is the counterpart of a string terminating on a monopole in particle physics [20]. In the NMR experiments, we guess that the hedgehog is created on the bottom (or top) wall of the container and moves up (or down) the vortex line, transforming one vortex into another (Fig. 7).

In the context of the electroweak model, transitions between vortices of different winding (topological charge) have been considered in Ref. [27].

4 Fermions and gauge fields

We now come to the second level of analogies as described in the beginning of Section 2. This is the analogy between the fermionic sector of the electroweak model and the interactions of quasiparticles in $^3\text{He-A}$ with the order parameter.

4.1 Fermionic sector of the electroweak model

The fermionic sector Lagrangian of the standard model of the electroweak interactions is as follows:

$$L_f = L_l + L_q \quad (4.1.1)$$

where, the lepton and quark sector Lagrangians for a single family are:

$$L_l = -i\bar{\Psi}\gamma^\mu D_\mu\Psi - i\bar{e}_R\gamma^\mu D_\mu e_R + h(\bar{e}_R\Phi^\dagger\Psi + \bar{\Psi}\Phi e_R) \quad (4.1.2)$$

$$L_q = -i(\bar{u}, \bar{d})_L\gamma^\mu D_\mu \begin{pmatrix} u \\ d \end{pmatrix}_L - i\bar{u}_R\gamma^\mu D_\mu u_R - i\bar{d}_R\gamma^\mu D_\mu d_R \\ -G_d \left[(\bar{u}, \bar{d})_L \begin{pmatrix} \phi^+ \\ \phi \end{pmatrix} d_R + \bar{d}_R(\phi^-, \phi^*) \begin{pmatrix} u \\ d \end{pmatrix}_L \right]$$

$$-G_u \left[(\bar{u}, \bar{d})_L \begin{pmatrix} -\phi^* \\ \phi^- \end{pmatrix} u_R + \bar{u}_R (-\phi, \phi^+) \begin{pmatrix} u \\ d \end{pmatrix}_L \right] \quad (4.1.3)$$

with $\phi^- = (\phi^+)^*$ and

$$\Psi = \begin{pmatrix} \nu \\ e \end{pmatrix}_L .$$

The indices L and R refer to left- and right-handed components.

In our analysis we will only be dealing with one fermion family at a time and hence we shall not be considering the effects of family mixing such as occurs due to the Kobayashi-Maskawa fermion mass matrix [28].

The covariant derivatives occurring in the electroweak Lagrangian are:

$$D_\mu \Psi = D_\mu \begin{pmatrix} \nu \\ e \end{pmatrix}_L = \left(\partial_\mu - \frac{i}{2} \tau^a W_\mu^a + \frac{i}{2} Y_\mu \right) \begin{pmatrix} \nu \\ e \end{pmatrix}_L \quad (4.1.4)$$

$$D_\mu e_R = (\partial_\mu + i Y_\mu) e_R \quad (4.1.5)$$

$$D_\mu \begin{pmatrix} u \\ d \end{pmatrix}_L = \left(\partial_\mu - \frac{i}{2} \tau^a W_\mu^a - \frac{i}{6} Y_\mu \right) \begin{pmatrix} u \\ d \end{pmatrix}_L \quad (4.1.6)$$

$$D_\mu u_R = \left(\partial_\mu - \frac{i2}{3} Y_\mu \right) u_R \quad (4.1.7)$$

$$D_\mu d_R = \left(\partial_\mu + \frac{i}{3} Y_\mu \right) d_R . \quad (4.1.8)$$

4.2 Fermions in ${}^3\text{He}$

In ${}^3\text{He-A}$, the fermion spectrum differs from that in the electroweak model. In place of the various quarks and leptons within a single family, there are only four species occurring as left and right weak doublets. One way to write these might be

$$\Psi_L = \begin{pmatrix} \nu \\ e \end{pmatrix}_L , \Psi_R = \begin{pmatrix} \nu \\ e \end{pmatrix}_R .$$

In this section we discuss how this is obtained.

The pair-correlated systems (superconductors and ${}^3\text{He}$ superfluids) in their unbroken state above T_c are Fermi liquids: they contain only interacting fermions. In terms of the field operator ψ_α for ${}^3\text{He}$ particles the action is

$$S = \int dt d^3x \left[\psi_\alpha^\dagger \left(i\partial_t - \frac{\vec{p}^2}{2m} + \mu \right) \psi_\alpha \right] + S_{int} , \quad (4.2.1)$$

where S_{int} includes the time-independent interaction of two particles (the quartic term), m is the mass of particle, $\vec{p} = -i\vec{\nabla}$ is the momentum and μ is the chemical potential. In general this system is described by the large number of fermionic degrees of freedom. However, as in the bosonic sector of ${}^3\text{He}$ described in Sec. 2.3, there are some simpler limiting cases.

(1) The hydrodynamic case describes the low-frequency motion of the system. In this case the system of interacting fermions can be described by only a few degrees of freedom corresponding to the slow collective motion: particle density n_N , spin density \vec{S} , mass velocity \vec{v} and entropy density S . Their dynamics is governed by the closed system of hydrodynamic equations.

(2) In the Fermi-gas limit - the limit of small particle-particle interaction - ${}^3\text{He}$ is a simple ensemble of noninteracting particles. For positive μ , the ground state is one in which all negative energy fermionic states (with $\vec{p}^2 < 2m\mu$) are occupied and corresponds to a *solid* Fermi sphere of radius $p_F = \sqrt{2m\mu}$.

(3) In the low-temperature limit, the large number of fermionic degrees of freedom of ${}^3\text{He}$ is effectively reduced and the system is well described as a system of noninteracting quasiparticles (dressed particles) which, according to Landau theory, occupies the same Fermi-sphere as a system of noninteracting particles. The particle-particle interaction simply renormalizes the effective mass and the magnetic moment of the quasiparticle. The residual interaction is reduced at low T because of the small number of thermal excitations above the Fermi-surface and can be neglected. Thus the action becomes

$$S = \int dt d^3x \psi_\alpha^\dagger [i\partial_t - \epsilon(\vec{p})] \psi_\alpha \quad , \quad (4.2.2)$$

where $\epsilon(\vec{p})$ is the quasiparticle energy spectrum. In a Fermi-liquid this description is valid in the so called degeneracy limit, when the temperature T is much smaller than the effective Fermi temperature $T_F \sim \hbar^2/(ma^2)$, where a is the interparticle distance. This situation takes place almost for all Fermi-systems above transition since $T_c \ll T_F$. Further for simplicity we use

$$\epsilon(\vec{p}) = p^2/(2m) - \mu \quad . \quad (4.2.3)$$

Below the superfluid/superconducting transition temperature T_c , new collective degrees of freedom appear, which are the order parameter fields, corresponding to the Higgs field in particle physics. The interaction of the

fermionic degrees of freedom (quasiparticles) with the order parameter in the broken symmetry state is described by the action:

$$S = \int dt d^3x \psi_\alpha^\dagger [i\partial_t - \epsilon(\vec{p})] \psi_\alpha + \frac{1}{2} \int dt d^3x d^3y [\psi_\alpha^\dagger(x) \psi_\beta^\dagger(y) \Delta_{\alpha\beta}(x, y) + \Delta_{\alpha\beta}^*(x, y) \psi_\beta(y) \psi_\alpha(x)] \quad (4.2.4)$$

In the BCS model this action is obtained from Eq.(4.2.1) in the limit when the particle-particle interaction is small and only that part of the interaction is left which leads to the formation of the order parameter. The quartic interaction in S_{int} is decomposed in a Hubbard-Stratonovich manner into the bilinear interaction given in eqn. (4.2.4) where a vacuum expectation value of the product of two annihilation operators

$$\Delta \propto \langle \text{vac} | \psi \psi | \text{vac} \rangle \quad , \quad (4.2.5)$$

represents the order parameter in the broken symmetry state. (Δ is a 2×2 matrix and is not to be confused with the gap amplitude Δ_0 of Sec. 2.). Δ breaks the $U(1)_N$ symmetry $\psi_\alpha \rightarrow e^{i\phi} \psi_\alpha$, since under $U(1)_N$ it transforms as $\Delta(x, y) \rightarrow e^{2i\phi} \Delta(x, y)$. If Δ has nontrivial spin and orbital structure, it also breaks the $SO(3)_L$ and $SO(3)_S$ symmetries.

The action in Eq.(4.2.4) allows transition between the states differing by two particles, say, N and $N - 2$. The order parameter Δ serves as the matrix element of such transition. This means that the single-fermion elementary excitation in the broken symmetry vacuum represents some mixture of the $N = 1$ (particle) and $N = -1$ (hole) states.

In electroweak theory the interactions corresponding to those in (4.2.4) are the Yukawa interactions between the left-handed $SU(2)_T$ doublets and the right-handed fermion singlets, which appear in the broken symmetry state (see Sec. (4.1)). An example of such an interaction is the term:

$$G_d(\bar{u}, \bar{d})_L \Phi d_R$$

in the electroweak Lagrangian. When Φ acquires a vacuum expectation value during the electroweak phase transition, this gives rise to the nonconservation of the isospin and hypercharge in the same manner as the charge N is not conserved in the broken symmetry action (4.2.4). These terms also lead to

the lepton and quark masses. In superfluids and superconductors these terms give rise to the gap in the quasiparticle spectrum.

In the electroweak vacuum one has many matrix elements $G_d\Phi$, $G_e\Phi$, $G_\mu\Phi$, $G_\tau\Phi$ etc. which give rise to masses of all quarks and leptons (except for the left-handed neutrino). All of them have the same symmetry structure. In condensed matter such a situation - with many symmetrically equivalent matrix elements in the broken symmetry state - is reminiscent of the situation in metals with several electron bands, $\epsilon_a(\vec{p})$, where a is the band index. In such metals, after the transition into the superconducting state, the matrix elements $\Delta_{aa'}$ appear between electrons and holes from different bands. All the elements are characterized by the same broken symmetry. However in most cases one can distinguish the matrix element $\Delta_{a_0a_0}$, actually the largest one, which is “primary”. This means that the symmetry breaking Cooper pairing occurs first between the electrons within the band $a = a_0$. This symmetry breaking induces the other (smaller) matrix elements Δ_{a_0a} and $\Delta_{aa'}$ with $a, a' \neq a_0$.

In some technicolour theories of the dynamical electroweak transition it was suggested that the “primary” matrix element is also the largest one, i.e. the symmetry breaking results from the “Cooper” pairing of the heaviest quarks and antiquarks (top quark condensate [29]), while the other (smaller) elements are induced by this symmetry breaking.

For the s -wave spin-singlet pairing in superconductors and the p -wave spin-triplet pairing in superfluid ${}^3\text{He}$ the matrix element has the following general form:

$$\Delta_{s\text{-wave}}(\vec{r}, \vec{p}) = i\sigma^{(2)}\Psi(\vec{r}) \quad , \quad (4.2.6)$$

$$\Delta_{p\text{-wave}}(\vec{r}, \vec{p}) = i\sigma^{(\mu)}\sigma^{(2)}A_{\mu i}(\vec{r})p_i/p_F \quad . \quad (4.2.7)$$

Here $\vec{\sigma}$ are the Pauli matrices in spin space, $\vec{r} = (\vec{x} + \vec{y})/2$ is the center of mass coordinate of the Cooper pair, while the momentum \vec{p} describes the relative motion of the two fermions within the Cooper pair: it is the Fourier transform of the coordinates $(\vec{x} - \vec{y})$. The complex scalar function $\Psi(\vec{r})$ and 3×3 matrix $A_{\mu i}(\vec{r})$ are the order parameters for the two systems. The symmetries of ${}^3\text{He}$ and the A-phase and the order parameter have been described in Sec. (2.1).

The easiest way to treat the action in Eq.(4.2.4), in which the states with 1 particle and -1 particle are hybridized by the order parameter, is to double the number of degrees of freedom introducing the antiparticle (hole) for each

particle. Let us introduce the Bogoliubov-Nambu field operator χ which is the spinor in this new particle-hole space:

$$\chi = \begin{pmatrix} \mathbf{u} \\ \mathbf{v} \end{pmatrix} = \begin{pmatrix} \Phi \\ i\sigma^{(2)}\Phi^\dagger \end{pmatrix} ; \quad \chi^\dagger = (\mathbf{u}^\dagger, \mathbf{v}^\dagger) . \quad (4.2.8)$$

It transforms under $U(1)_N$ symmetry operation $\Phi_\alpha \rightarrow e^{i\phi}\Phi_\alpha$ as

$$\chi \rightarrow e^{i\tilde{\tau}_3\phi}\chi , \quad (4.2.9)$$

where $\tilde{\tau}_i$ are Pauli matrices in the Nambu space, such that $\tilde{\tau}_3$ is the operator \mathbf{N} for quasiparticles with the eigenvalue $+1$ for the particle and -1 for the hole.

The eigenvalue equation for the quasiparticle spectrum is

$$\mathcal{H}\chi = E\chi , \quad (4.2.10)$$

with the Hamiltonian

$$\mathcal{H}_{s\text{-wave}} = \epsilon(\vec{\mathbf{p}})\tilde{\tau}_3 + \begin{pmatrix} 0 & \Psi(\vec{r}) \\ \Psi^*(\vec{r}) & 0 \end{pmatrix} . \quad (4.2.11)$$

in s -wave superconductors, and,

$$\mathcal{H}_{A\text{-phase}} = \epsilon(\vec{\mathbf{p}})\tilde{\tau}_3 + \frac{\Delta_0}{p_F}(\vec{\sigma} \cdot \hat{\mathbf{d}})(\tilde{\tau}_1\hat{e}_1(\vec{r}) \cdot \vec{\mathbf{p}} - \tilde{\tau}_2\hat{e}_2(\vec{r}) \cdot \vec{\mathbf{p}}) , \quad (4.2.12)$$

in the A-phase of ${}^3\text{He}$.

The square of the fermion energy

$$E_{s\text{-wave}}^2(\vec{p}) = \mathcal{H}^2 = \epsilon^2(\vec{p}) + |\Psi|^2 , \quad (4.2.13)$$

$$E_{A\text{-phase}}^2(\vec{p}) = \mathcal{H}^2 = \epsilon^2(\vec{p}) + \left(\frac{\Delta_0}{p_F}\right)^2(\vec{p} \times \hat{\mathbf{I}})^2 , \quad (4.2.14)$$

together with (4.2.3), shows that the fermions in the s -wave system have a gap in the spectrum, while in the A-phase, if the chemical potential μ is positive, the quasiparticle spectrum has two zeros (nodes): at $\vec{p} = \pm p_F \hat{\mathbf{I}}$. These nodes are the source of anomalies in ${}^3\text{He-A}$.

In the vicinity of each zero the spectrum of the fermions is relativistic and from Eq.(4.2.12) it follows

$$\mathcal{H} = \sum_{N=1}^3 e_N^j \tilde{\tau}_N (p_j - q_A A_j) , \quad (4.2.15)$$

where $\vec{A} = p_F \hat{\mathbf{l}}$ plays the role of a vector potential like an “electromagnetic” field, q_A is the corresponding “electric” charge which is +1 for the fermions in the vicinity of the node $\vec{p} = p_F \hat{\mathbf{l}}$ and -1 for the fermions in the vicinity of the opposite node at $\vec{p} = -p_F \hat{\mathbf{l}}$. The coefficients e_N^i are

$$\vec{e}_1 = 2S_3 \frac{\Delta_0}{p_F} \hat{e}_1 , \quad \vec{e}_2 = -2S_3 \frac{\Delta_0}{p_F} \hat{e}_2 , \quad \vec{e}_3 = q_A v_F \hat{\mathbf{l}} , \quad (4.2.16)$$

where $v_F = p_F/m$ is the Fermi velocity; the quantum number $S_3 = \pm 1/2$ is the spin projection of the fermions on the axis $\hat{\mathbf{d}}$.

The coefficients e_N^i form the so called *dreibein*, or triad, the local coordinate frame for the fermionic particles. They are the 3-dimensional version of the *vierbein* or tetrads, which are used to describe gravity in the tetrad formalism of general relativity. From Eq.(4.2.16) it follows that $\det[e_N^i]$ has the sign of q_A , *i.e.* the A -charge, q_A , also defines the parity of the fermions: the fermions with positive q_A are right-handed and those with negative q_A are left-handed.

The conventional metric tensor expressed in terms of the triad e_N^i is

$$g^{ij} = \sum_{N=1}^3 e_N^j e_N^i , \quad (4.2.17)$$

so the square of the energy of fermions in the vicinity of each of the nodes is

$$E^2(\vec{p}) = g^{ij} (p_i - q_A A_i) (p_j - q_A A_j). \quad (4.2.18)$$

Eq.(4.2.15) is the Weyl Hamiltonian for charged chiral particles: the positively charged left handed fermions are concentrated near the momentum $\vec{p} = p_F \hat{\mathbf{l}}$, while the negatively charged right handed fermions are concentrated near the momentum $\vec{p} = -p_F \hat{\mathbf{l}}$. Note that the metric is flat if $\hat{\mathbf{l}}$ is constant.

Note also the close analogy of eqn. (4.2.15) with the interaction of the electroweak Z -field with the fermions. For example, if we set all other gauge

fields (A , W_1 and W_2) to zero, the interaction of the left- and right-handed electrons with the Z field is given by

$$-i\bar{e}_L\gamma^\mu\left(\partial_\mu + \frac{i}{2}\cos(2\theta_w)Z_\mu\right)e_L - i\bar{e}_R\gamma^\mu\left(\partial_\mu + \frac{i}{2}(\cos(2\theta_w) - 1)Z_\mu\right)e_R .$$

For $\sin^2\theta_w = 0.25$ – which is quite close to the observed value of 0.23 – even the Z charges of the left- and right-handed electrons are related by a minus sign.

4.3 Bosonic sector of ${}^3\text{He-A}$ on Level 2 of analogy

In spite of the similarity between $\vec{A} = p_F\hat{\mathbf{I}}$ in Eq. (4.2.15) and the Z gauge field, \vec{A} is closer to the *massless* electromagnetic field A , than to the *massive* Z -field. The $\hat{\mathbf{I}}$ -vector is a dynamical field: the propagating oscillations of $\hat{\mathbf{I}}(\vec{r}, t)$ (the so called orbital waves) have the massless spectrum of the photons[1].

It should be mentioned that the “electromagnetic” field \vec{A} and “electric” charge e on this Level 2 of analogies has nothing to do with the “electric” charge of the analogy at Level 1. On Level 1 the “electromagnetic” field is absent, since the $U(1)_Q$ group is global. On Level 2 the “gauge” field $\vec{A} = p_F\hat{\mathbf{I}}$ is a part of the order parameter whose action on the fermions is like the action of the electromagnetic field on the fermions in the electroweak model. Actually $\vec{A} = p_F\vec{l}$ corresponds to an axial field since it acts in opposite ways on left-handed and right-handed fermions.

On Level 1 of the analogy, the W -bosons should be related to the $SO(3)_L$ group, but they are absent because this group is global. However, on Level 2 the electroweak W bosons arise [1]. The 2 additional gauge fields W^1 and W^2 , corresponding to the W -bosons which are transverse to the $\hat{\mathbf{d}}$ (i.e. $\hat{\mathbf{d}} \cdot \vec{W} = 0$) enter the Hamiltonian for fermions, if one considers the effect of the spin $\vec{\sigma}$ of the ${}^3\text{He}$ atoms and of the other (non-Goldstone) degrees of the order parameter

$$A_{\mu i} = (A - \text{phase vacuum}) + \delta A_{\mu i} . \quad (4.3.1)$$

As a result the Hamiltonian for fermions is

$$\mathbf{H} = \sum_{N=1}^3 e_N^i \check{\tau}_N (p_i - q_A A_i - q_W \check{\sigma}_\alpha W_i^\alpha) . \quad (4.3.2)$$

Here $q_W = q_A$; the components of the W_i^α field are related to $\delta A_{\alpha i} = u_{\alpha i} + i v_{\alpha i}$ in the following way:

$$W_x^\alpha + i W_y^\alpha = i(p_F/\Delta_A) e^{\alpha\beta\gamma} \hat{d}^\beta \delta A_{\gamma z} \quad . \quad (4.3.3)$$

So only 4 components of W_i^α are nonzero:

$$W_x^1 = v_{yz} p_F \quad , \quad W_x^2 = -v_{xz} p_F \quad , \quad W_y^1 = -u_{yz} p_F \quad , \quad W_y^2 = u_{xz} p_F \quad , \quad (4.3.4)$$

which corresponds to the gauge field produced by the transverse W -bosons. The contribution to the longitudinal W^3 -bosons is absent in the p -wave order parameter $A_{\alpha i}$.

There are altogether 18 real elements of the 3×3 matrix $A_{\alpha i}$: 4 of them correspond to W -bosons; 2 - to electromagnetic field (photons), 3 to gravitons, while the other 9 have no analogy in electroweak interactions.

The electromagnetic and the W -boson sector of ${}^3\text{He-A}$ in this Level 2 analogy has the form

$$L_W + L_A = m_W^2 W_{\mu a} W^{\mu a} - \frac{1}{4g^2} W_{\mu\nu a} W^{\mu\nu a} - \frac{1}{4e^2} A_{\mu\nu} A^{\mu\nu} \quad , \quad (4.3.5)$$

where m_W is the mass of the W boson and $g = e$ which corresponds to the weak mixing angle $\theta_W = \pi/2$. Both charges e and g experience the zero-charge effect due to the screening polarization of the fermion vacuum: as $T \rightarrow 0$ one has $e^2 = g^2 \propto 1/\ln \frac{\Lambda_0}{T}$ which results in the logarithmic divergence of the gradient energy in Eq.(2.3.5). This is different from the standard model, where the charge g experiences the asymptotic freedom. This is because in ${}^3\text{He-A}$ the charged W -bosons do not contribute to the renormalization of g .

Note that the metric g_{ij} appearing in (4.2.17) appears to be related to the electromagnetic potential A_i in (4.2.15). But this relationship is only valid on the vacuum manifold. If we consider small oscillations of all 18 components of the order parameter, i.e. including the non-Goldstone modes, we find that the ‘‘gravitational’’ waves and the ‘‘electromagnetic’’ waves are independent, at least for propagation along $\hat{\mathbf{l}}$. In this case, the gravitons are (massive) oscillations of $g_{11} - g_{22}$ and g_{12} and are unrelated to the (massless) oscillations of $\hat{\mathbf{l}}$. So while there are similarities on this **Level 2** of analogies, there are some differences too which one must bear in mind.

5 Anomalies

5.1 Baryon number anomaly in the electroweak model

In the electroweak model described in Section (4.1) there are additional accidental global symmetries that are present. These are the $U(1)_B$ and $U(1)_L$ symmetries whose classically conserved charges are baryon number and lepton number. Each of the quarks is assigned $1/3$ baryon number and zero lepton number while the leptons (neutrino and electron in Section (4.1)) are assigned lepton number 1 and zero baryon number.

The conservation of baryon number (B) and lepton number (L) is anomalous and the current conservation equations are:

$$\partial_\mu j_B^\mu = \partial_\mu j_L^\mu = \frac{N_F}{32\pi^2} \left(-W_{\mu\nu}^a \tilde{W}^{a\mu\nu} + Y_{\mu\nu} \tilde{Y}^{\mu\nu} \right) \quad (5.1.1)$$

where, N_F is the number of families and the dual of the field strength is defined by $\tilde{F}^{\mu\nu} = \frac{1}{2}\epsilon^{\mu\nu\lambda\sigma}F_{\lambda\sigma}$. Note that $B - L$ is still conserved but $B + L$ is not. The nonconservation results from the spectral flow of the chiral massless fermions in the presence of the field strength because the left-handed and right-handed fermions in Eqs.(4.1.4-8) have different charges.

In the case of the electroweak strings the spectral flow is provided by the fermion zero modes localized on strings. If we consider a configuration of electroweak Z -string loops, the direct integration of the macroscopic anomaly equation (5.1.1) gives the following change in baryon number between two string configurations [4]:

$$\Delta B = 2N_F \cos(2\theta_w) \Delta L . \quad (5.1.2)$$

where, ΔL is the change in the linking number of the strings. This result can be derived in a more rigorous microscopic theory by considering the spectrum of fermions in a string background and by working out the quantum numbers of the ground state of the fermions. This calculation was done in Ref. [5] by properly regularizing the divergent terms. However the calculation for the similar phenomenon in ${}^3\text{He}$ (see Sec. (6.7) below) suggests that the macroscopic result is true only in the limit of large B .

The origin of the non-trivial baryon number of linked loops of string is due to an Aharonov-Bohm interaction of the fermionic zero modes on one

loop with the other linked loop. This interaction shifts the energy levels of the fermions and leads to non-trivial quantum numbers.

Below we consider the similar effects in the $^3\text{He-A}$ texture (Sec.5.2), where the macroscopic anomaly equation of the type of Eq.(5.1.1) is used, and within the core of vortices (Sec.6), where the microscopic analysis of the fermionic zero modes is presented.

5.2 Mass current anomaly in $^3\text{He-A}$

The axial anomaly is a consequence of the spectral flow of fermions: if the fermions are gapless, the inhomogeneous vacuum induces a spectral flow, which carries particles from negative energy states of the vacuum to positive energy states. As a result, the corresponding conserved quantity (viz, charge) is transferred from a coherent vacuum motion into incoherent fermionic degrees of freedom, which is visualized as creation of charge from the vacuum. It was shown in [30, 31] that the same phenomenon takes place in superfluid $^3\text{He-A}$, where the gap in the quasiparticle spectrum has point nodes. This results in a spectral flow of fermionic quasiparticles through the nodes when the condensate evolves in time. Since the left-handed and right-handed fermions have opposite linear momentum an immediate result of this effect is the linear momentum (or mass current) anomaly in $^3\text{He-A}$.

The mass density ρ in superfluid ^3He is equal to the bare mass m_3 of ^3He atom times the particle density

$$\rho(\vec{r}, t) = m_3 \langle \text{vac} | \Phi_\alpha^\dagger \Phi_\alpha | \text{vac} \rangle , \quad \int d^3r \rho(\vec{r}, t) = m_3 \langle \text{vac} | \mathbf{N} | \text{vac} \rangle . \quad (5.2.1)$$

Using Eq.(4.2.8) the particle density can be also represented in terms of the Bogoliubov-Nambu field χ and the charge N operator $\tilde{\tau}_3$:

$$\Phi_\alpha^\dagger \Phi_\alpha = \frac{1}{2} \chi^\dagger \tilde{\tau}_3 \chi , \quad (5.2.2)$$

the factor $1/2$ compensates for the double counting in the description in terms of particles and holes. If all the fermionic excitations of superfluid vacuum are massive (i.e. there are no nodes), the slow dynamics of the superfluids or superconductors at zero temperature is the dynamics of the collective variable (the order parameter field and the density ρ) since the fermionic quasiparticles are not created. The mass (particle) conservation law (which

comes from the $U(1)_N$ symmetry of physical laws) is thus exhausted by the collective (hydrodynamic) variables:

$$\partial_t \rho + \vec{\nabla} \cdot \vec{j} = 0 \quad , \quad (5.2.3)$$

where the mass current (or the density of linear momentum) in the nodes-free superfluids is

$$\vec{j}_{\text{node-free}} = \rho \vec{v}_s + \frac{1}{2} \vec{\nabla} \times \vec{\mathbf{L}} \quad . \quad (5.2.4)$$

Here \vec{v}_s is the superfluid velocity. The first term in (5.2.4) is the zero temperature limit of (2.1.8a): the density ρ_n of the thermal fermionic excitations is zero at $T = 0$. The second term is the orbital current originating from the internal angular momentum of the liquid. The vector $\hat{\mathbf{L}}$ is the density of the angular momentum. For the hypothetical nodes-free A-phase state (i.e. for $\mu < 0$) the symmetry $\mathbf{Q} = \mathbf{L}_3 - (1/2)\mathbf{N} \equiv \mathbf{L} \cdot \hat{\mathbf{1}} - (1/2)\mathbf{N}$ of the vacuum requires that the angular momentum density equals 1/2 of particle density, since the charge Q of the vacuum is zero:

$$\vec{\mathbf{L}}_{\text{node-free}} = \frac{\hbar}{2m_3} \rho \hat{\mathbf{1}} \quad . \quad (5.2.5)$$

The gap nodes, via the axial anomaly, modify the equation (5.2.4) for the mass current. Also the vacuum can accumulate the charge Q of gapless fermions, which leads to the nonzero charge Q of the vacuum. As a result the angular momentum can deviate from its fundamental form in Eq.(5.2.5).

The gapless chiral fermions in Eq.(4.2.15) obey the same Adler-Bell-Jackiw anomaly equation [32, 33] which gave rise to Eq.(5.1.1) for the baryonic and leptonic charges. Here we are interested only in the effect produced by the ‘‘gauge’’ field $\vec{A} = p_F \hat{\mathbf{1}}$:

$$\partial_t Q_c = \frac{1}{2\pi^2} \int d^3r (\partial_t \vec{A} \cdot (\vec{\nabla} \times \vec{A})) \quad , \quad (5.2.6)$$

where $Q_c = \int d^3r \delta S / \delta A_0$ is the chiral charge of the fermions. This anomaly equation describes the production of the chiral charge in ${}^3\text{He-A}$ during the dynamics of the order parameter $\vec{A} = p_F \hat{\mathbf{1}}$.

Since each created left fermion carries the linear momentum $p_F \hat{\mathbf{1}}$ and the same momentum is carried by the created left antifermion, the total production of the quasiparticle linear momentum is[30]:

$$\partial_t \vec{P}_{qp} = \frac{1}{2\pi^2} \int d^3r p_F \hat{\mathbf{1}} (\partial_t \vec{A} \cdot (\vec{\nabla} \times \vec{A})) \quad . \quad (5.2.7)$$

This is a linear momentum anomaly in $^3\text{He-A}$.

Since the total linear momentum is nevertheless conserved, Eq.(5.2.7) means that momentum is transferred from the collective variables describing the inhomogeneous vacuum to the system of quasiparticles.

This equation allows us to calculate the extra mass current of the $\hat{\mathbf{l}}$ texture due to accumulation of the fermionic charge by the texture, which would correspond to the baryonic charge in Eq.(5.1.2) accumulated by the inhomogeneous vacuum of Z -string. Let us take the arbitrary but fixed $\hat{\mathbf{l}}(\vec{r})$ texture and consider the process in which the node-free A-phase transforms to the “real” A-phase, that is, the phase with nodes. This occurs if the Fermi momentum changes from $p_F = 0$ at $t = t_0$ to its equilibrium value in the real A-phase. In this process $\partial_t \vec{A} = \hat{\mathbf{l}} \partial_t p_F$. The total momentum of the texture thus changes according to Eq.(5.2.7):

$$\vec{P}(t) - \vec{P}(t_0) = - \int_{t_0}^t dt \partial_t \vec{P}_{qp} = - \frac{1}{6\pi^2} \int d^3r p_F^3 \hat{\mathbf{l}} (\hat{\mathbf{l}} \cdot (\vec{\nabla} \times \hat{\mathbf{l}})) , \quad (5.2.8)$$

where $\vec{P}(t_0)$ is the anomaly-free momentum

$$\vec{P}(t_0) = \int d^3r \vec{j}_{\text{node-free}} . \quad (5.2.9)$$

The mass current in the A-phase (the momentum density) thus becomes

$$\vec{j} = \vec{j}_{\text{node-free}} + \vec{j}_{\text{anomalous}} = \rho \vec{v}_s + \frac{1}{2} \vec{\nabla} \times \frac{\rho \hat{\mathbf{l}}}{2m_3} - \frac{\hbar}{2m_3} C_0 \hat{\mathbf{l}} (\hat{\mathbf{l}} \cdot (\vec{\nabla} \times \hat{\mathbf{l}})) \quad (5.2.10)$$

where, $C_0 = m_3 p_F^3 / 3\pi^2$. The extra mass current results from the helicity of the \vec{A} field:

$$\vec{j}_{\text{anomalous}} = - \frac{1}{6\pi^2} p_F \hat{\mathbf{l}} (\vec{A} \cdot (\vec{\nabla} \times \vec{A})) , \quad (5.2.11)$$

in the same manner as the baryonic charge of string is the consequence of the helicity of the gauge fields [4].

5.3 Momentum exchange between the moving continuous vortex and heat bath.

The axial anomaly results in a curious exchange of the linear momentum between the moving texture and the heat bath. Let us consider this on

the example of the $n = 2$ continuous vortex discussed in Sec.(3.3). When this vortex moves with velocity \vec{v}_L , the $\hat{\mathbf{1}}$ -texture becomes time dependent: $\hat{\mathbf{1}} = \hat{\mathbf{1}}(\vec{r} - \vec{v}_L t)$. As a result the “electric” field arises

$$\vec{E} = \partial_t \vec{A} = p_F \partial_t \hat{\mathbf{1}} = -p_F (\vec{v}_L \cdot \vec{\nabla}) \hat{\mathbf{1}} , \quad (5.3.1)$$

According to the anomaly equation (5.2.7) this leads to the production of quasiparticle momentum. This momentum is absorbed by the normal component of the liquid (the heat bath) moving with the velocity \vec{v}_n . This means that there appears a (reactive, i.e. nondissipative) force between the vortex and the heat bath caused by the spectral flow of the fermions. The force acting per unit length of the vortex is

$$\vec{F}_{\text{spectral flow}} = \frac{1}{2\pi^2} \int dx dy p_F^3 \hat{\mathbf{1}} \left(((\vec{v}_L - \vec{v}_n) \cdot \vec{\nabla}) \hat{\mathbf{1}} \cdot (\vec{\nabla} \times \hat{\mathbf{1}}) \right) , \quad (5.3.2)$$

Here \vec{v}_n enters since for this effect the heat bath reference frame is the relevant frame for the vortex motion.

Simple transformation of this equation using the integration by parts gives [34]

$$\vec{F}_{\text{spectral flow}} = \frac{C_0}{2m_3} (\vec{v}_L - \vec{v}_n) \times \hat{z} \int dx dy \hat{\mathbf{1}} \cdot (\partial_x \hat{\mathbf{1}} \times \partial_y \hat{\mathbf{1}}) . \quad (5.3.3)$$

Finally using the Eq.(3.3.2) one obtains the anomaly contribution to the force acting on the $n = 2$ vortex:

$$\vec{F}_{\text{spectral flow}} = 2C_0 \vec{\kappa} \times (\vec{v}_n - \vec{v}_L) . \quad (5.3.4)$$

This force does not depend on the details of the vortex structure and is defined by the anomaly parameter C_0 in Eq.(5.2.10) and by the winding number n of the vortex. This stresses the topological origin of this anomalous force.

In the following Section it will be shown that the same type of anomaly (and the same force) arises for vortices in any Fermi superfluid or superconductor, even if they do not contain the gap nodes in homogeneous state. For conventional singular vortex, say, in s -wave superconductor, the effect occurs because the quantized vortex itself, due to its singularity at the vortex axis, plays the same role as gap nodes in A-phase of ^3He [35]. The microscopic

analysis shows that the vortex gives rise to the fermion zero modes in the vortex core, whose spectral flow is responsible for the anomalous force. The result of this microscopic calculation agrees with Eq.(5.3.4) obtained from the macroscopic anomaly equation, but only in a special limit.

6 Fermions on vortices and strings

6.1 Symmetry generators

Let us consider singular vortices in the s -wave superconductors and in the A-phase, and singular Z -strings in the electroweak vacuum (Eq.(2.3.7)). Here we are interested in the simplest vortices, which display the cylindrical symmetry. The asymptotical behavior of the order parameter far from the vortex core of coherence length size ($\xi(T) \sim 1/m_{Higgs}(T)$ in electroweak theory) is

$$\Phi_{\text{ew}}(r \rightarrow \infty) = \frac{\eta}{\sqrt{2}} e^{in\phi} \begin{pmatrix} 0 \\ 1 \end{pmatrix} , \quad (6.1.1a)$$

$$\vec{\Psi}_{3\text{He-A}}(r \rightarrow \infty) = e^{in\phi} \frac{\hat{x} + i\hat{y}}{\sqrt{2}} , \quad (6.1.1b)$$

$$\Psi_{s\text{-wave}}(r \rightarrow \infty) = \Delta_0 e^{in\phi} . \quad (6.1.1c)$$

All these linear defects have an integer winding number n , except for the Alice string in the A-phase, which has $n = \pm 1/2$. In the A-phase and electroweak vacuum these linear defects have a constant $\hat{\mathbf{I}} = \vec{z}$; the vortices and strings, which correspond to each other, have the following relation between their winding numbers: $n_{Z\text{-string}} = (1/2)n_{\text{vortex}}$. This means that a 4π $^3\text{He-A}$ vortex corresponds to a 2π Z -string (both are topologically unstable and can transform to the disgyration in the $\hat{\mathbf{I}}$ field with winding number $n = 2$). For the 2π -vortex and for the π -vortex (the Alice string) there are no counterparts in the electroweak vacuum. The Alice string exists in the A-phase, only if one takes into account the total order parameter including the spin degrees of freedom (see eqn.(3.1.5b)). The asymptotic form of the order parameter for the 2π vortex is given in eqn. (3.1.5a).

The electroweak Z -string in Eq.(6.1.1a), in addition to the translational symmetry along the vortex axis with the generator $\vec{\mathbf{p}}_z$, has two continuous symmetries given by the following generators:

$$\mathbf{Q} = \mathbf{T}_3 + (1/2)\mathbf{Y} , \quad \mathbf{Q}_n = \mathbf{L}_3 - n\mathbf{Y} ; \quad (6.1.2a)$$

where $\mathbf{L}_3 = -i\partial_\phi$ is the generator of the coordinated rotations.

For vortices in conventional superconductors one also has two generators:

$$\mathbf{Q}_n = \mathbf{L}_3 - \frac{n}{2}\mathbf{N} \quad , \quad \mathbf{S}_3 \quad ; \quad (6.1.2b)$$

Here \mathbf{S}_3 is the generator of the $SO(3)_S$ rotation group, which is not broken in s -wave superconductors.

Two generators also take place in the axisymmetric A-phase vortices with integer winding number n :

$$\mathbf{Q}_n = \mathbf{L}_3 - \frac{n + \hat{l}_z(\infty)}{2}\mathbf{N} \quad , \quad \mathbf{S}_3 \quad , \quad n = \text{integer} \quad ; \quad (6.1.2c)$$

Here $\hat{l}_z(\infty) = \pm 1$ gives the orientation of $\hat{\mathbf{l}}$ vector at infinity; \mathbf{S}_3 is the generator of the $SO(2)_S$ rotations about the vector $\hat{\mathbf{d}}$, i.e. of the little group of the broken symmetry group $SO(3)_S$ in Eq.(2.1.1b), and, \mathbf{L}_3 includes both the coordinate rotations $-i\partial_\phi$ and internal rotations of the orbital part of the order parameter $\vec{\Psi}$ (see Eq.(3.1.8)). (Remember that in ^3He , orbital rotations in $SO(3)_L$ are not just rotations in “internal” space as in the electroweak model; instead these are rotations in physical space as well (see eqn. (3.1.8c)). Then, axial symmetry implies that the z -component of $\hat{\mathbf{l}}$ is ± 1 at infinity.)

For the Alice strings in $^3\text{He-A}$, *i.e.* vortices with half integer winding number, one has only one generator, since the orbital and spin degrees of freedom are coupled topologically:

$$\mathbf{Q}_n = \mathbf{L}_3 + \frac{1}{2}\mathbf{S}_3 - \frac{n + \hat{l}_z(\infty)}{2}\mathbf{N} \quad , \quad n = \pm 1/2 \quad . \quad (6.1.2d)$$

These symmetries, if they are not spontaneously broken in the vortex core, also define the vortex structure in the core. For example, Eq.(6.1.2b) implies that the order parameter for the symmetric vortex in the s -wave superconductor is everywhere described by one radial function

$$\Psi_{s\text{-wave}}(\vec{r}) \equiv \Delta(\vec{r}) = |\Delta(r)|e^{in\phi} \quad , \quad (6.1.3)$$

while the symmetric A-phase vortex in Eq.(3.1.5c) contains 2 radial functions.

For typical vortices realized and observed in superfluid ^3He phases some of the vortex symmetries are spontaneously broken, including the continuous symmetries. The breaking of axial symmetry in the vortex core was

experimentally observed in $^3\text{He-B}$ vortices due to the new Goldstone mode [36]. In cosmic strings the analogous spontaneous breaking of the continuous symmetry in the vortex core has been discussed by Witten [37]. In this case the spontaneously broken symmetry is the electromagnetic symmetry $U(1)_Q$ with the generator \mathbf{Q} in Eq.(6.1.2a), which implies the appearance of superconductivity within the core of the string with a nondissipative current along the vortex axis.

6.2 Fermion Zero Modes and Symmetry of the Vortex

The existence of low-energy fermions (“zero modes”) in a vortex background can be deduced by the application of certain index theorems which relate the number of such modes to the vortex winding number n . Originally this relation was found for the fermionic spectrum localized on strings in particle physics [38, 39].

The spectrum of single-fermionic excitations in a vortex,

$$E_{n_r}(p_z, Q, Q_n, S_3, \dots)$$

depends on the momentum projection p_z on the vortex axis (a continuous quantum number), and on the discrete eigenvalues of the generators of continuous symmetry: these quantum numbers can be integer or half integer. n_r here is the radial quantum number, and is not due to any symmetry of the system.

In relativistic theories the number of branches $E(p_z)$ crossing $E = 0$ as functions of p_z equals n (see Fig. 8a for $n = 1$). For fermions in condensed matter vortices there is no such theorem. However a similar theorem exists if one considers the spectrum as a function of the generalized angular momentum Q_n in Eqs.(6.1.2b-d) Fig. 8b-d. The interlevel distance of bound states $\partial E_{Q_n}/\partial Q_n = \omega_0$ is small compared to the gap amplitude $\Delta_0(T)$ of fermions in bulk: $\omega_0 \sim \Delta_0^2(T)/E_F \ll \Delta_0(T)$. Thus, if one neglects the interlevel distance as compared, say, with temperature or with the level width, the spectrum can be considered as a continuous function of the *continuous* parameter Q_n . As a function of continuous Q_n the spectrum has anomalous (chiral) branches, fermion zero modes, $E_0(p_z, Q_n)$ whose number N_{zm} is related to the vortex winding number $N_{\text{zm}} = 2N$ according to the index theorem [35]. As a function of Q_n , each anomalous branch crosses zero of

energy an odd number of times and runs through both discrete and continuous spectrum from $E_0 = -\infty$ to $E_0 = +\infty$. Any other branch either does not cross zero of energy at all or crosses it an even number of times. For low-energy bound states, the spectrum of the chiral branch is linear in Q_n . For the most symmetric vortices, for example,

$$E_0(p_z, Q_n) = Q_n \omega_0(p_z) \quad . \quad (6.2.1)$$

In the next subsection this will be derived in a simplified way with the aid of the quasiclassical approximation valid in the limit $Q \gg 1$, ie in the range where we can consider Q_n as continuous variable. Thus, in the limit of large Q_n , when Q_n can be considered as a continuous coordinate in the 2D momentum space (Q_n, p_z) , the fermions occupying the negative energy levels form a 2D Fermi liquid. The role of the Fermi surface is played by the line $Q_n = 0$, at which the energy spectrum crosses zero.

However, as was found in original paper [40] for *s*-wave superconductors, the Eq.(6.2.1) is valid even for small Q_n , where the discrete nature of Q_n becomes important. If one is interested in the fine energy scale of the order or less than the interlevel distance ω_0 , one again comes to the problem of existence of the gap nodes in the spectrum as function of p_z . Three different types (a-c) of the behavior of the fermionic spectrum in the low-energy limit are possible (Fig.8 b-c) [41]. One of the factors which determines the behavior of the spectrum at low energy is the following property of the quantum number Q_n of the fermions: Q_n can be either half-integer or integer depending on the vortex symmetry. It appears that for conventional $n = 1$ vortices in *s*-wave superconductors the quantum number Q_n is half-integer. Then, according to the Eq.(6.2.1) the case (a) occurs: there is a finite gap $E(Q = 1/2, p_z = 0) = \omega_0/2$ in the fermionic spectrum (Fig. 8b).

In the most symmetric $^3\text{He-A}$ vortices the orbital momentum Q_n is integer. This leads to a possibility of the case (b): the branch with $Q_n = 0$ represents the flat band with zero energy: $E(Q_n = 0, p_z) \equiv 0$ for all p_z (Fig.8d). Existence of such flat band is supported by the symmetry of the vortex and is also confirmed in exact calculations [42] of the fermion spectrum.

In the most symmetric $^3\text{He-B}$ vortex the symmetry, which leads to zero energy at $Q_n = 0$, takes place only at $p_z = 0$. This produces the case (c): One or more branches of the spectrum with particular Q_n 's (in our case with

$Q_n = 0$) cross the zero level as functions of p_z (Fig.8c). In this case the fermions occupying negative energy levels form 1D Fermi liquids, in which Fermi surfaces are reduced to a Fermi point $p_z = 0$. This is very similar to the fermion zero modes in cosmic strings.

Which of three types (a-c) of the behavior of the fermionic spectrum is realized depends first on the property of Q_n . In Eq.(6.1.2b) the quantity Q_n for the single-particle fermionic excitation is integer, if the winding number n is even, or half-of-odd-integer if n is odd (note that the eigenvalues of \mathbf{N} are $N = 1$ for particle and $N = -1$ for the hole).

The state with a vortex line can also possess discrete symmetries [12, 41]. In the most symmetric vortices these are space inversion symmetry \mathbf{P} , and combined \mathbf{TU}_2 symmetry which corresponds to the overturn of the vortex axis with the simultaneous time inversion, the circulation being unchanged under this combined operation. One more important symmetry is related to the structure of Bogoliubov fermions: this is the symmetry under the operation \mathbf{C} of transformation of Bogoliubov particle into Bogoliubov hole. Transformations of the quasiparticle spectrum under these operations are [11]:

$$\begin{aligned}\mathbf{C}E(Q_n, p_z) &= -E(-Q_n, -p_z) \ , \\ \mathbf{P}E(Q_n, p_z) &= E(Q_n, -p_z) \ , \\ \mathbf{TU}_2E(Q_n, p_z) &= E(Q_n, p_z) \ ,\end{aligned}\tag{6.2.2}$$

where $E(Q_n, p_z)$ denotes the whole set of eigenvalues corresponding to given Q and p_z .

If \mathbf{CP} symmetry is satisfied one has

$$E_a(Q_n, p_z) = -E_b(-Q_n, p_z) \ ,\tag{6.2.3}$$

which means that for the state a with given Q_n and p_z one can find another state b which has opposite energy E for opposite Q and the same p_z . Just this symmetry together with the index theorem give the Eq. (6.2.1) for the fermions on the vortex with $n = 1$ in s -wave superconductor. Indeed, the index theorem implies that the number of the low-lying branches of fermions in terms of the continuous momentum Q_n is n for each spin projection. This means that in the $n = 1$ vortex there is the only branch for each of two spin quantum numbers $S_z = \pm 1/2$. Since different spin projections do not mix

(we neglect here the spin-orbit interaction), it follows from Eq.(6.2.2) that each branch is an odd function of Q_n :

$$E_{\uparrow}(Q_n, p_z) = -E_{\uparrow}(-Q_n, p_z) \quad , \quad E_{\downarrow}(Q_n, p_z) = -E_{\downarrow}(-Q_n, p_z) \quad , \quad (6.2.3)$$

and one obtains the Eq.(6.2.1), where Q_n now is the discrete variable. The factor $\omega_0(p_z)$ is known from the semiclassical limit of large Q_n .

The Eq.(6.2.1) can be interpreted as the interaction of the orbital momentum $\vec{Q} = Q_n \hat{z}$ of the localized fermion with the internal ‘‘magnetic’’ field $\vec{h}(p_z) = \omega_0(p_z) \hat{z}$, produced by the vortex:

$$E = \vec{Q} \cdot \vec{h}(p_z) \quad . \quad (6.2.4)$$

If the quasiparticle orbital momentum is zero, its energy is exactly zero.

This is not the case for the $n = 1$ vortex in s -wave superfluids or superconductors, where Q_n can only be half-of-odd-integer, which results in the gap. This small gap in the spectrum can be in principle reduced by some extra perturbations, such as crystal field, spin-orbit interaction, external magnetic field, etc.

6.3 Fermion Zero Modes in semiclassical approach

The existence of fermionic zero modes does not depend on the details of the system and is completely defined by topology. So here we will consider the simplest and best known case of an axisymmetric singular vortex in superfluid or superconductor with s -wave pairing. The orbital quantum number Q_n is considered here as a continuous variable and so one can use the quasiclassical approximation for the fermions localized in the vortex core. The Bogoliubov Hamiltonian for the fermions with given spin projection is a 2×2 matrix

$$\mathcal{H} = \check{\tau}_3 \vec{q} \cdot (-i \vec{\nabla}) / m + \check{\tau}_1 \text{Re} \Delta(\vec{r}) - \check{\tau}_2 \text{Im} \Delta(\vec{r}) \quad . \quad (6.3.1)$$

Here $\vec{q} = \vec{p} - \hat{z}(\vec{p} \cdot \hat{z})$ is the quasiparticle momentum in the transverse plane and $\Delta(\vec{r}) = e^{in\phi} |\Delta(r)|$ is the gap function (order parameter) in the axisymmetric vortex with winding number n .

The quantum numbers, which characterize the fermionic levels in this approximation, are (i) the magnitude of transverse momentum of quasiparticle q , which is related to the longitudinal projection of momentum $q^2 = p_F^2 - p_z^2$,

(ii) the radial quantum number n_r and (iii) the continuous impact parameter $y = \hat{z} \cdot (\vec{r} \times \vec{q})/q$. It is related to the angular momentum $\hbar Q_n$ by $Q_n = qy$. Introducing the coordinate $x = \vec{r} \cdot \vec{q}/q$ along \vec{q} , such that $r^2 = x^2 + y^2$, and assuming that in the important regions one has $|y| \ll |x|$, one obtains the dependence of the gap function in the singly-quantized vortex ($n = 1$) on x and y :

$$\Delta(\vec{r}) \approx |\Delta(|x|)|(\text{sign}(x) - i\frac{y}{|x|}) \quad , \quad (6.3.2)$$

and the Hamiltonian:

$$\mathcal{H} = \mathcal{H}^{(0)} + \mathcal{H}^{(1)} \quad ,$$

$$\mathcal{H}^{(0)}(x) = -i\check{\tau}_3 \frac{q}{m} \nabla_x + \check{\tau}_1 |\Delta(|x|)| \text{sign}(x) \quad , \quad \mathcal{H}^{(1)}(x, y) = \check{\tau}_2 y \frac{|\Delta(|x|)|}{|x|} \quad . \quad (6.3.3)$$

The Hamiltonian $\mathcal{H}^{(0)}(x)$ is “supersymmetric” - there is an operator $\check{\tau}_2$ which anticommutes with $\mathcal{H}^{(0)}(x)$, i.e. $\{\mathcal{H}^{(0)}, \tau_2\} = 0$, and it has an integrable eigenfunction corresponding to zero eigenvalue:

$$\mathcal{H}^{(0)}\Psi^{(0)}(x) = 0 \quad , \quad \Psi^{(0)}(x) \propto (\check{\tau}_0 - \check{\tau}_2) \exp \left[-\frac{m}{q} \int_0^{|x|} dr |\Delta(r)| \right] \quad . \quad (6.3.4)$$

Here $\check{\tau}_0$ is the diagonal 2×2 matrix.

Using first order perturbation theory in $\mathcal{H}^{(1)}$ one obtains the lowest energy levels:

$$E(n_r = 0, Q_n, p_z) \approx \langle 0 | \mathcal{H}^{(1)} | 0 \rangle = -y \langle \frac{|\Delta(r)|}{r} \rangle = -Q_n \omega_0(p_z) \quad , \quad (6.3.5)$$

$$\omega_0(p_z) = \frac{1}{q(p_z)} \frac{\int_0^\infty dr |\Psi^{(0)}(r)|^2 |\Delta(r)|/r}{\int_0^\infty dr |\Psi^{(0)}(r)|^2} \quad . \quad (6.3.6)$$

This is the anomalous branch of the low-energy localized fermions obtained in Ref. [40]. If the energy spectrum is considered as a continuous function of Q_n , this anomalous branch crosses zero at $Q_n = 0$.

6.4 Spectral Flow in Vortices: Callan-Harvey mechanism of anomaly cancellation

Now let us consider again the force, which arise when the vortex moves with respect to the heat bath. In Sec.5.3 we discussed this for the special case

of the continuous ${}^3\text{He-A}$ vortex where the macroscopic Adler-Bell-Jackiw anomaly equation could be used. Now we consider this effect using the microscopic description of the spectral flow of fermion zero modes within the vortex core. We show that the same force arises for any vortex in any superfluid or superconductor under a special condition.

If the vortex moves with the velocity \vec{v}_L with respect to the heat bath, the coordinate \vec{r} is replaced by the $\vec{r} - \vec{v}_L t$ and the impact parameter y which enters the quasiparticle energy in Eq.(6.3.5) shifts with time. So the energy becomes

$$E_{n,r=0}(Q_n, p_z, t) = -(y - \frac{\epsilon(\vec{q})}{q}t)q\omega_0(p_z) = -(Q_n - \epsilon(\vec{q})t) \omega_0(p_z) . \quad (6.4.1)$$

Here $\epsilon(\vec{q}) = \hat{z} \cdot (\vec{v}_L \times \vec{q})$ acts on fermions localized in the core in the same way that an electric field acts on the fermions localized on a string in relativistic quantum theory. The only difference is that under this “electric” field the spectral flow occurs in the Q_n direction rather than along p_z . Along this path the fermionic levels cross the zero energy level at the rate

$$\partial_t Q_n = \epsilon(\vec{q}) = \hat{z} \cdot (\vec{v}_L \times \vec{q}) . \quad (6.4.2)$$

This leads to the quasiparticle momentum transfer from the vacuum (from the levels below zero) along the anomalous branch into the heat bath. This occurs at the rate

$$\partial_t \vec{P} = \sum_{\vec{p}} \vec{p} \partial_t Q_n = \frac{1}{2} N_{\text{zm}} \int_{-p_F}^{p_F} \frac{dp_z}{2\pi} \int_0^{2\pi} \frac{d\phi}{2\pi} \vec{q} \epsilon(\vec{q}) = \pi n \frac{p_F^3}{3\pi^2} \hat{z} \times \vec{v}_L, \quad (6.4.3)$$

where the factor $\frac{1}{2}$ compensates the double counting of particles and holes, and we used the index theorem that the number of anomalous branches (fermion zero modes) is related to the winding number: $N_{\text{zm}} = 2n$. This gives the force acting on the vortex when it moves with respect to the heat bath:

$$\vec{F}_{\text{spectral flow}} = \kappa n \hbar C_0 \hat{z} \times (\vec{v}_n - \vec{v}_L) , \quad C_0 = \frac{m_3 p_F^3}{3\pi^2} . \quad (6.4.4)$$

Here \vec{v}_n is the velocity of the heat bath, which in equilibrium coincides with the velocity of the normal component of the liquid consisting of the thermal excitations.

Here it is implied that all the quasiparticles, created from the negative levels of the vacuum state, finally become part of the normal component, i.e. there is nearly reversible transfer of linear momentum from fermions to the heat bath. This should be valid in the limit of large scattering rate: $\omega_0\tau \ll 1$, where τ is the lifetime of the fermion on the Q_n level. This condition, which states that the interlevel distance on the anomalous branch is small compared to the life time of the level, is the crucial requirement for spectral flow to exist. In the opposite limit $\omega_0\tau \gg 1$ the spectral flow is suppressed and the corresponding spectral flow force is exponentially small [43]. This shows the limitation for exploring the macroscopic Adler-Bell-Jackiw anomaly equation (Eq.(5.1.1)) in the electroweak model and Eq. (5.2.7) in ${}^3\text{He-A}$.

The reactive force $\vec{F}_{\text{spectral flow}}$ from the heat bath on the moving vortex is the consequence of the reversible flux of momentum from the vortex into the region near the axis, i.e. into the core region. Within the core the linear momentum of the vortex transforms to the linear momentum of the fermions in the heat bath when the fermionic levels on anomalous branches cross the chemical potential.

The process of transfer of linear momentum from the superfluid vacuum to the normal motion of fermions within the core is the realization of the Callan-Harvey mechanism for anomaly cancellation [44]. In the case of the condensed matter vortices the anomalies - nonconservation of linear momentum both in the one-dimensional world of the vortex core fermions and in the three-dimensional Bose-condensate outside the vortex core - compensate each other. This is the same kind of the Callan-Harvey effect which has been discussed in Sec.(5.3) for the motion of continuous textures in ${}^3\text{He-A}$. ${}^3\text{He-A}$ is, however, a very special superfluid, since due to its internal topology it always contains the gap nodes in the spectrum. The nodes lead to momentum nonconservation, if one considers the superfluid condensate motion alone. This is the result of the transfer of momentum to the normal fermionic system due to the level flow through the gap nodes. As distinct from ${}^3\text{He-A}$, where the gap nodes are always present, the Callan-Harvey effect for vortices occurs in any Fermi-superfluid: the anomalous fermionic Q branch, which mediates the momentum exchange, always appears in the singular or continuous core, due to nontrivial topology of the quantized vortex. This type of Callan-Harvey effect does not depend on the detailed structure of the vortex core and even on the type of pairing, and is defined by the vortex winding

number n . Thus it is the same for the singular and continuous vortices, if the condition $\omega_0\tau \ll 1$ is fulfilled.

This force appears to be similar to the Magnus force - the hydrodynamic force acting on the vortex with the winding number n moving in the ideal liquid (see below). However there is a great difference between two forces. While the Magnus force \vec{F}_{Magnus} is also proportional to the winding number n , it corresponds to the hydrodynamic momentum transfer between different parts of the vacuum: it describes the momentum exchange between the coherent motion of the inhomogeneous vacuum (the moving vortex) and the mass flow in the vacuum at infinity. This does not depend on the fermionic background. On the contrary, $\vec{F}_{\text{spectral flow}}$ describes the momentum exchange between the coherent motion of the inhomogeneous vacuum (vortex) and the fermionic degrees of freedom. It disappears if the level flow is suppressed. In the Bose superfluids, like superfluid ^4He , the $\vec{F}_{\text{spectral flow}}$ is completely absent: there are no fermions. It is also absent in the node-free A-phase, where the anomaly parameter $C_0 = 0$.

6.5 Three reactive forces acting on a moving vortex

There are 3 different velocities, which are relevant for vortex motion: the superfluid velocity \vec{v}_s (or the velocity of the vacuum) far from the vortex; the velocity of the heat bath \vec{v}_n ; and the velocity of the vortex line \vec{v}_L . As a result, in general there are 3 different nondissipative forces acting on the vortex, which we discuss below.

Here we assume that the condition $\omega_0\tau \ll 1$ for the spectral flow is fulfilled. It is important that in this limit case the dissipative (drag or frictional) forces can be neglected [43]. The three nondissipative forces are as follows:

$$\vec{F}_{nd} = \vec{F}_{\text{Magnus}} + \vec{F}_{\text{Iordanskii}} + \vec{F}_{\text{spectral flow}} \quad , \quad (6.5.1)$$

$$\vec{F}_{\text{Magnus}} = n\vec{\kappa} \times \rho(\vec{v}_L - \vec{v}_s) \quad , \quad (6.5.2)$$

$$\vec{F}_{\text{Iordanskii}} = n\vec{\kappa} \times \check{\rho}_n(T)(\vec{v}_s - \vec{v}_n) \quad , \quad (6.5.3)$$

$$\vec{F}_{\text{spectral flow}} = n\vec{\kappa} \times C_0(\vec{v}_n - \vec{v}_L) \quad . \quad (6.5.4)$$

Each of the three forces is of topological origin.

(i) According to the Landau picture of the superfluid liquid (see Sec.2.1), Eqs.(2.1.6-7)), its motion consists of the motion of the superfluid vacuum

(with the total mass density ρ and the superfluid velocity \vec{v}_s) and the dynamics of the elementary excitations. The Magnus force in Eq. (6.5.1) acts on the vortex if it moves with respect to the superfluid vacuum. As before n is the vortex winding number, $\vec{\kappa}$ is the circulation vector: for the Fermi (Bose) superfluids $\kappa = \pi\hbar/m$ ($\kappa = 2\pi\hbar/m$), m is the bare mass of the fermion (boson). In Eqs.(6.5.2-3) \vec{v}_s is the vacuum (superfluid) velocity far from the vortex where the $1/r$ contribution from the velocity field circulating around the vortex can be neglected. The Magnus force comes from the flux of linear momentum from the vortex to infinity. The topological origin of this force in condensed matter was discussed in Refs.[45, 46].

(ii) The Iordanskii force [47, 48] results from the elementary excitations outside the vortex core: the vortex line produces for them the Aharonov-Bohm potential. This force can be obtained as a sum of the forces acting on the individual particles according to the equation

$$\partial_t \vec{p} = (\vec{\nabla} \times \vec{v}_s) \times \vec{p},$$

where \vec{p} is the quasiparticle momentum and the vorticity $\vec{\nabla} \times \vec{v}_s = n\vec{\kappa}\delta_2(\vec{r})$ is concentrated in a thin tube (vortex core). The Iordanskii force is thus

$$-\sum_{\vec{p}} f \partial_t \vec{p} = -n\vec{\kappa} \times \int \frac{d^3p}{4\pi^3} f[E_{\vec{p}} + \vec{p} \cdot (\vec{v}_s - \vec{v}_n)] = n\vec{\kappa} \times \check{\rho}_n(T)(\vec{v}_n - \vec{v}_s).$$

Here f is Fermi or Bose function depending on the type of the elementary excitations, which is Doppler shifted due to the counterflow $\vec{v}_n - \vec{v}_s$; and $\check{\rho}_n(T)$ is the density of the normal component, which can be an anisotropic tensor. The Iordanskii force is the only nondissipative force in Eq.(6.5.1), which depends on temperature T .

In the next subsection we will discuss the analogy of the Iordanskii effect with the Aharonov-Bohm effect for a spinning cosmic string [49]. Note that the Iordanskii force, though related to the particles surrounding the string, is not the drag (frictional) force on the string from the particles. As distinct from the drag force, the Iordanskii force is invariant under the time reversal and thus is nondissipative.

The Aharonov-Bohm interaction of particles with cosmic strings was discussed in [50]. But for conventional (nonspinning) strings it gives rise only to the frictional drag force, which should be added to the drag force caused by to the scattering of particles off the core of the string [51]. In condensed

matter vortices the drag force is small in the considered limit $\omega_0\tau \ll 1$ and is neglected here. For the global relativistic string the sum of the nondissipative Magnus and Iordanskii type forces was discussed in [52] and it was found that they arise only if the string is spinning.

(iii) The third term in Eq. (6.5.1) exists only in fermionic systems, where the fermion zero modes can exist. It was found recently that the spectral flow is unaffected by the temperature T , since the temperature does not change the topology of the spectrum of fermion zero modes, and thus the parameter C_0 equals its zero temperature value in Eq.(6.4.4) [53]. In the real Fermi-superfluids the existence of $\vec{F}_{spectral\ flow}$ is defined by the condition $\omega_0\tau \ll 1$. At low T this condition can be violated and the discrete character of the spectrum suppresses the level flow, as a result this force disappears [54], while the Magnus force always survives. On the other hand, if the anomalous force exists, it nearly compensates the Magnus force, since in the real superfluids the mass density ρ is very close to the anomaly parameter $C_0 = m_3 p_F^3 / (3\pi^2)$. That is why the anomaly within the core plays a very important part in the vortex dynamics.

In $^3\text{He-B}$ the anomalous (spectral flow) contribution to the force has been experimentally observed. When the temperature increases the regime of the suppressed spectral flow transfers to the regime where it nearly compensates the Magnus force [43]. This behavior reproduces the measured temperature dependence of the force acting on the vortex [55].

6.6 Aharonov-Bohm effect and analog of the spinning string

To clarify the analogy between the Iordanskii force and Aharonov-Bohm effect, let us consider the simplest cases of phonons propagating in the velocity field of the quantized vortex in the Bose superfluid ^4He and fermions propagating in the velocity field of the quantized vortex in the Fermi superfluid $^3\text{He-A}$. According to Unruh [56] the dynamics of the phonons in the presence of the velocity field is the same as the dynamics of photons in the gravity field. For the velocity field of quantized vortex the phonons obey the equation

of motion of the scalar wave in the metric

$$ds^2 = (c^2 - v_s^2(r)) \left(dt + \frac{n\kappa}{2\pi(c^2 - v_s^2(r))} d\phi \right)^2 - dr^2 - dz^2 - \frac{c^2}{c^2 - v_s^2(r)} r^2 d\phi^2 . \quad (6.6.1)$$

Here c is the sound velocity, $\vec{v}_s = n\hat{\phi}\kappa/(2\pi r)$ is the superfluid velocity around the vortex, and we use the cylindrical system of coordinates with the axis z along the vortex line.

The same metric takes place for the gapless Bogoliubov fermions propagating in the field of the axisymmetric phase vortex with $\hat{\mathbf{l}} = \hat{z}$ in the A-phase of superfluid ^3He [34]. Let us consider how the Lagrangian for the fermions

$$\mathcal{L} = -i\partial_t + \mathcal{H} \quad (6.6.2)$$

with \mathcal{H} from Eq.(4.2.12) is modified in the presence of the superfluid velocity \vec{v}_s of the vortex. This potential flow can be gauged out by applying the gauge transformation in Eq.(4.2.9) to the Lagrangian. In the vicinity of the nodes this gives:

$$\mathcal{L} = \sum_{N=1}^4 \tilde{\tau}_N e_N^\mu (p_\mu - eA_\mu) , \quad (6.6.3)$$

where the vierbein give the following metric tensor

$$g^{\mu\nu} = -e_0^\mu e_0^\nu + \sum_{N=1}^3 e_N^\mu e_N^\nu , \quad (6.6.4)$$

with the components

$$g^{ij} = \sum_{N=1}^3 e_N^j e_N^i = c_{\parallel}^2 \hat{\mathbf{l}}_i \hat{\mathbf{l}}_j + c_{\perp}^2 (\delta_{ij} - \hat{\mathbf{l}}_i \hat{\mathbf{l}}_j) - v_{(s)i} v_{(s)j} , \quad g^{00} = -1 , \quad g^{0i} = v_{(s)i} \quad (6.6.5)$$

In this case the “velocity of light” is anisotropic and its transverse component $c_{\perp} = \Delta_0/p_F$ enters Eq. (6.6.1) if only the motion in the transverse plane is considered.

Far from the vortex, where $v_s(r)$ is small and can be neglected, this metric corresponds to that of the so called spinning cosmic string. The spinning cosmic string (see the recent references [57, 58]) is a string which has rotational angular momentum. The metric in Eq. (6.6.1) corresponds to

a string with angular momentum $J = n\kappa/(8\pi G)$ per unit length and with zero mass.

The effect peculiar to the spinning string is the gravitational Aharonov-Bohm topological effect [49]. Though the metric outside the string is flat, there is a time difference for the particles propagating around the spinning string in opposite directions. For the vortex (at large distances from the core) this time delay approaches

$$2\tau = \frac{2n\kappa}{c^2} . \quad (6.6.6)$$

This asymmetry between the particles moving on different sides of the vortex is just the origin of the Iordanskii force acting on the vortex in the presence of the net momentum of the quasiparticles: $2 \int d^3p/(2\pi)^3 \vec{p}f(\vec{p})$.

6.7 Angular momentum anomaly

As distinct from the linear momentum, the orbital angular momentum projection L_3 and the generalized angular momentum Q_n in the axisymmetric environment are quantized integer or half of odd integer quantities and they can serve as a model for the quantized and integer baryonic charge in electroweak theory.

The symmetry Q_n of different inhomogeneous but axisymmetric vacua in Eqs.(6.1.2) tells us that Q_n is a conserved quantity. Moreover, since Q_n is the sum of the generator which correspond to the particle number, angular and spin momenta, the charge Q_n is integer (or half of odd integer) quantum number from the very beginning. Thus the correct calculations of the total charge of the whole system (vacuum plus excitations) should also give integer or half integer value.

Eq.(6.1.2) does not mean, however, that the Q_n -charge of the vacuum is always zero. In the pure fermionic description the total charge of the vacuum is

$$\langle \text{vac} | \mathbf{Q}_n | \text{vac} \rangle = \sum_{Q_n, p_z, n_r} Q_n \Theta(-E_{n_r}(p_z, Q_n)) \quad (6.7.1)$$

where $E_{n_r}(p_z, Q_n)$ are the energy eigenvalues of Eq.(4.2.10) for fermions in the axisymmetric field of the order parameter, $\Theta(-E_{n_r}(p_z, Q_n))$ is the Heaviside function which restricts the sum so that only the negative energy states con-

tribute to the vacuum charge. The Q_n charge of the vacuum can be nonzero if some discrete symmetry is broken and $E_{n_r}(p_z, Q_n) \neq E_{n_r}(p_z, -Q_n)$.

An example of nonzero vacuum charge is presented by ferromagnets, where the $SO(3)$ spin rotation symmetry is broken to $SO(2)$. So the spin projection S_3 is a good quantum number (charge). The absence of the time-inversion symmetry leads to the net charge $\langle \text{vac} | \mathbf{S}_3 | \text{vac} \rangle \neq 0$ of the vacuum, which corresponds to the spontaneous magnetic moment of the ferromagnet.

Let us consider the Q_n -charge of the continuous $n = 2$ vortex in Eq.(3.3.1) for which $\hat{l}_z(\infty) = -1$. Then according to Eq. (6.1.2c) this charge corresponds to the “electric” charge $Q = L_3 - (1/2)N$ of the homogeneous vacuum in which the vector $\hat{\mathbf{I}}$ is oriented along $\hat{\mathbf{I}}(r = 0) = \hat{z}$. This is a consequence of the fact that the $n = 2$ vortex can be continuously transformed to this homogeneous vacuum state. For simplicity the function $\alpha(r)$, which enters the axisymmetric ansatz for the $n = 2$ vortex in Eq. (3.3.1) will be considered as a constant.

First we use the macroscopic (hydrodynamic) description in terms of the anomaly equation. In this approach, the orbital momentum L_3 of the vacuum state is the momentum of the mass current \vec{j} in Eq.(5.2.10):

$$\langle \text{vac} | \mathbf{L}_3 | \text{vac} \rangle = \int d^3r \hat{z} \cdot (\vec{r} \times \vec{j}) . \quad (6.7.2)$$

For the axisymmetric texture, Eq. (2.1.10) for the superfluid vorticity is simplified:

$$\vec{\nabla} \times \vec{v}_s = -\frac{\kappa}{2\pi r} \hat{z} \partial_r \cos \eta . \quad (6.7.3)$$

and can be integrated, to obtain the velocity distribution in terms of the $\hat{\mathbf{I}}$ texture. The resulting velocity field without singularity on the axis (at $r = 0$) is:

$$\vec{v}_s = \hat{\phi} \frac{\kappa}{2\pi r} (1 - \cos \eta) , \quad (6.7.4)$$

which requires $\hat{\mathbf{I}}(r = 0) = \hat{z}$.

The integration of the first two (regular) terms in Eq.(5.2.10), after integration by part and using the boundary condition $\rho(R) = 0$ (there are no particles outside the vessel of radius R), gives the contribution to $\langle \text{vac} | \mathbf{L}_3 | \text{vac} \rangle$:

$$\frac{1}{2m_3} \int d^3r \rho(r) = \frac{1}{2} N = \frac{1}{2} \langle \text{vac} | \mathbf{N} | \text{vac} \rangle . \quad (6.7.5)$$

Here N is the total number of particles.

As a result the charge $Q_n = L_3 - (1/2)N$ of the vacuum is given by the last term in the current which resulted from the anomaly equation (5.2.7):

$$\begin{aligned} \langle \text{vac} | \mathbf{Q}_n | \text{vac} \rangle &= -\frac{1}{2} \int d^3r C_0 (\hat{z} \cdot (\vec{r} \times \hat{\mathbf{I}})) (\hat{\mathbf{I}} \cdot (\vec{\nabla} \times \hat{\mathbf{I}})) \\ &= -\pi L \int_0^R dr r^2 C_0 \sin^2 \alpha \sin \eta \left(\partial_r \eta + \frac{\sin \eta \cos \eta}{r} \right), \end{aligned} \quad (6.7.6)$$

where L is the height of the vessel and R its radius.

Thus the vacuum accumulates nonzero Q_n charge only if the $\hat{\mathbf{I}}$ texture contains helicity, $(\hat{\mathbf{I}} \cdot (\vec{\nabla} \times \hat{\mathbf{I}})) \neq 0$, in complete correspondence with the baryonic charge accumulated by the helical gauge fields [4]. The helicity of the $\hat{\mathbf{I}}$ texture is nonzero only for $\sin \alpha \neq 0$:

$$\hat{\mathbf{I}} \cdot (\vec{\nabla} \times \hat{\mathbf{I}}) = \sin \alpha \left(\partial_r \eta + \frac{\sin \eta \cos \eta}{r} \right). \quad (6.7.7)$$

Also, $\sin \alpha$ is nonzero only if the parities \mathbf{P} ($\vec{r} \rightarrow -\vec{r}$) and PTU_2 are broken (T is the time inversion symmetry and U_2 is the rotation by π about transverse axis, see Eq.(6.2.2)).

One also can rewrite this Q_n -charge of the vacuum using the axial anomaly equation. Again one considers the process in which the $\hat{\mathbf{I}}$ -texture is constant, but the parameter p_F changes from zero at $t = t_0$ (when $p_F = 0$, the axial field $\vec{A} = p_F \hat{\mathbf{I}} = 0$ and the Q_n charge of the vacuum is zero) to its equilibrium value at present time t :

$$\langle \text{vac} | \mathbf{Q}_n | \text{vac} \rangle = -\frac{1}{2\pi^2} \int d^3r \int_{t_0}^t dt Q_n(\vec{r}, t) (\partial_t \vec{A} \cdot (\vec{\nabla} \times \vec{A})). \quad (6.7.8)$$

The integrand describes the transfer of the chiral charge from the vacuum to the chiral fermionic quasiparticles. Each created left fermion carries (at the moment of creation) the local charge $Q_n(\vec{r}, t)$ within the semiclassical (macroscopic) description of the fermions.

Actually on the microscopic level this transfer of the charge Q_n should occur in quantum steps at the moment when the fermionic level crosses zero energy. Thus one obtains an integer value (or half integer, if the vortex is singly quantized), which in the limit of large Q_n transforms to the macroscopic expression (6.7.6).

Let us consider how this occurs at large Q_n . We consider the evolution of the Q_n charge of the vacuum during the change of the texture from the initial state with $\alpha = 0$ (and $Q_n = 0$) to the final state with finite α . During the evolution of the vortex structure, Q_n levels cross the zero energy and this leads to the accumulation of the charge Q_n in the vacuum. The rate of the charge Q_n production can be found from the following consideration. In the limit of large Q_n the spectrum $E(Q_n, p_z)$ crosses zero as a function of Q_n at some $Q_n(p_z)$. This function $Q_n(p_z)$ changes in the process of the modification of the vortex. Since the states with $Q_n > Q_n(p_z)$ have positive (negative) energy while the states with $Q_n < Q_n(p_z)$ have negative (positive) energy, the change of $Q_n(p_z)$ induces the flow of the Q_n levels through zero with the rate $\partial_t Q_n(p_z)$. Since at each event the charge $Q_n(p_z)$ is transferred from the vacuum to the fermionic degrees of freedom, the total rate of the charge transfer is

$$\partial_t \langle \text{vac} | \mathbf{Q}_n | \text{vac} \rangle = \sum_{p_z} Q_n(p_z) \partial_t Q_n(p_z) . \quad (6.7.9)$$

Thus if one starts from the most symmetric vortex and continuously transfers this state into the vortex with broken symmetry, one obtains the following general result for the charge Q_n of the vortex:

$$\langle \text{vac} | \mathbf{Q}_n | \text{vac} \rangle = \frac{1}{2} \sum_{p_z} Q_n^2(p_z) . \quad (6.7.10)$$

This is valid for any axisymmetric vortex in any superfluid and superconductor.

For the continuous $n = 2$ vortex [59]

$$Q_n(p_z) = r(p_z) \sin \alpha \sqrt{p_F^2 - p_z^2} , \quad (6.7.11)$$

where $r(p_z)$ is the radius at which

$$\cos \eta(r) = \frac{p_z}{p_F} . \quad (6.7.12)$$

The energy levels with the lowest $|E_{n_r}(p_z, Q_n)|$ correspond to the radial quantum $n_r = 0$ and are given by

$$E(Q_n, p_z) = \frac{\Delta_0}{p_F r(p_z) \cos \alpha} (Q_n - Q_n(p_z)) . \quad (6.7.13)$$

Though Q_n is discrete, the distance between the Q_n levels $\Delta_0/(p_F r(p_z) \cos \alpha)$ is very small compared with the gap amplitude Δ_0 , which means that the effective Q_n is large and can be considered as continuous. Calculating the sum in Eq.(6.7.10) using the Eq.(6.7.11) one reproduces the macroscopic result in Eq.(6.7.6) [60].

7 Conclusions

In this article, we have discussed various aspects of ${}^3\text{He}$ and pointed out the similarities to the standard electroweak model of particle physics. These analogies occur on the level of symmetry groups and also on the interaction of fermions with the order parameter. We have discussed the topological defects that exist in ${}^3\text{He-A}$ and have been observed in the laboratory. The $n = 2$ vortex in ${}^3\text{He}$ is directly analogous to the Z -string in the electroweak model. The similarity in the interactions of fermions with the order parameter leads to similar anomalies in the two systems. In the electroweak model, baryon number conservation is anomalous while in ${}^3\text{He}$ the conservation of angular momentum - without accounting for the angular momentum of the quasiparticles - is anomalous. The presence of the anomaly can also be deduced from the existence of fermionic zero modes in both systems.

While there are striking similarities between the two systems, there are some obvious differences too that cannot be ignored. A crucial difference at the level of symmetries is that the symmetries in ${}^3\text{He}$ are global but those in the standard model are gauged. The fermionic degrees of freedom too are very different - the standard model has three families each of which has 15 fermions (including the color degree of freedom) while ${}^3\text{He}$ only has 4 fermions. In any case, we do not expect the analogy between the two systems to be exact. But the presence of certain similarities in itself should be useful to address certain field theoretic questions arising in one system in the context of the other system. For example, calculations in the condensed matter literature show that the change in the anomalously conserved angular momentum is always an integer [60] while corresponding calculations in the particle physics literature find a non-integer value [61, 5]. We feel that the analogy between the two systems could be exploited to resolve such issues. In addition, advantage could be taken of the experiments currently being performed on ${}^3\text{He}$. For example, according to [43], the linear momentum

anomaly caused by the spectral flow of fermions in the vortex has recently been observed in $^3\text{He-B}$ by measuring the temperature dependence of the force acting on moving vortices [55] (see Sec. (6.5)).

Acknowledgements:

We thank A. Achúcarro, M.B. Hindmarsh, T.W.B. Kibble, N.B. Kopnin, M. Krusius and N. Turok for illuminating discussions. We also thank M. Krusius, Ü. Parts and V. Ruutu for presenting their experimental results [24, 25] prior to publication and E. Thuneberg for his permission to use some of his Figures. This work was triggered by the activity during the Topological Defects program at the Isaac Newton Institute and would not have been done had it not been for this impetus. G.E.V. was supported through the ROTA co-operation plan of the Finnish Academy and the Russian Academy of Sciences and by the Russian Foundation for Fundamental Sciences, Grant Nos. 93-02-02687 and 94-02-03121. T.V. was supported in the early stages of this work by a Rosenbaum Fellowship at the Isaac Newton Institute.

References

- [1] G. E. Volovik, *Exotic properties of superfluid ^3He* , World Scientific, Singapore - New Jersey - London - Hong Kong, 1992.
- [2] Y. Nambu, Nucl. Phys. **B130**, 505 (1977).
- [3] T. Vachaspati, Phys. Rev. Lett. **68**, 1977 (1992); **69**, 216(E) (1992); Nucl. Phys. **B397**, 648 (1993).
- [4] T. Vachaspati and G.B. Field, Phys. Rev. Lett. **73**, 373 (1994); **74**, *Errata* (1995).
- [5] J. Garriga and T. Vachaspati, Nucl. Phys. **B438**, 161 (1995).
- [6] T. Vachaspati and A. Achúcarro, Phys. Rev. **D44**, 3067 (1991).
- [7] L.I. Burlachkov and N.B. Kopnin, Sov. Phys. JETP **65**, 630 (1987).
- [8] N.D. Mermin and T.-L. Ho, *Phys. Rev. Lett.*, **36**, 594 (1976).
- [9] D. Vollhardt and P. Wölfle, *The Superfluid Phases of ^3He* , (Taylor & Francis, London, 1990).
- [10] A. Schwarz, Nucl. Phys., **B 208**, 141 (1982).
- [11] M. Khazan, JETP Lett., **41**, 486 (1985).
- [12] M. M. Salomaa and G. E. Volovik, Rev. Mod. Phys., **59**, 533 (1987).
- [13] J. March-Russel, J. Preskill and F. Wilczek, Phys. Rev. Lett. **68**, 2567 (1992); A.C. Davis, A.P. Martin, Nucl. Phys. **B 419**, 341 (1994).
- [14] G.E. Volovik and V.P. Mineev, *ZhETF*, **72**, 2256 (1977); [*Sov. Phys.: JETP* **45**, 1186 (1977)].
- [15] S.G. Naculich, Phys. Rev. Lett. **75**, 998 (1995).
- [16] P.W. Anderson and G. Toulouse, *Phys. Rev. Lett.*, **38**, 508 (1977); V.R. Chechetkin, *ZhETF*, **71**, 1463 (1976); [*JETP*, **44**, 766 (1976)].

- [17] S. Blaha, *Phys. Rev. Lett.*, **36**, 874 (1976); G.E. Volovik and V.P. Mineev, *Pis'ma ZhETF*, **23**, 647 (1976); [*JETP Lett.*, **23** 593 (1976)].
- [18] V.M.H. Ruutu, Ü. Parts, J.H. Koivuniemi, M. Krusius, E.V. Thuneberg and G.E. Volovik, *Pis'ma ZhETF* **60**, 659 (1994) [*JETP Lett.* **60**, 671 (1994)].
- [19] Yu.G. Makhlin and T. Sh. Misirpashaev, *Pis'ma ZhETF* **61**, 48 (1995) [*JETP Lett.* **61**, 49 (1995)].
- [20] A. Vilenkin and E.P.S. Shellard, "Cosmic Strings and Other Topological Defects", Cambridge University Press (1994).
- [21] Ü. Parts, J.M. Karimäki, J.H. Koivuniemi, M. Krusius, V.M.H. Ruutu, E.V. Thuneberg and G.E. Volovik, "Phase diagram of vortices in rotating superfluid $^3\text{He-A}$ ", *Phys. Rev. Lett.*, **75** issue 16 (1995).
- [22] J. Preskill, *Phys. Rev.* **D46**, 4218 (1992).
- [23] E.V. Thuneberg, *Physica*, **B 210**, 287 (1995); M. Heinilä and G.E. Volovik, *Physica*, **B 210**, 300 (1995); Ü. Parts, V.M.H. Ruutu, J.H. Koivuniemi, M. Krusius, E.V. Thuneberg and G.E. Volovik, *Physica*, **B 210**, 311 (1995).
- [24] V.V. Avilov, M. Krusius, Ü. Parts, V.M.H. Ruutu and G.E. Volovik, to be published.
- [25] Ü. Parts, M. Krusius and V.M.H. Ruutu, to be published.
- [26] N.D. Mermin, in *Quantum Fluids and Solids* ed. by S.B. Trickey, E.D. Adams and J.W. Dufty (Plenum, New York), p.3 (1977)
- [27] A. Achúcarro, R. Gregory, K. Kuijken and J. Harvey, *Phys. Rev. Lett.* **72**, 3646 (1993).
- [28] T.P. Cheng and L.F. Li, "Gauge Theories of Elementary Particle Physics", Oxford University Press (1991).
- [29] S.F. King, *Rep. Prog. Phys.*, **58**, 263 (1995).

- [30] G.E. Volovik, *Pis'ma ZhETF*, **43**, 428 (1986) [*JETP Lett.* **43**, 551 (1986)].
- [31] M. Stone and F. Gaitan, *Ann. Phys.*, **178**, 89 (1987).
- [32] S. Adler *Phys. Rev.*, **177**, 2496 (1969).
- [33] J.S. Bell and R. Jackiw, *Nuovo Cim.*, **A 60**, 47 (1969).
- [34] G.E. Volovik, *ZhETF*, **102**, 1838 (1992); [*JETP* , **75**, 990 (1992)].
- [35] G.E. Volovik, *Pis'ma ZhETF*, **57**, 233 (1993); [*JETP Lett.*, **57**, 244 (1993)].
- [36] Y. Kondo, J.S. Korhonen, M. Krusius, V.V. Dmitriev, Yu.M. Mukharskiy, E.B. Sonin and G.E. Volovik, *Phys. Rev. Lett.*, **67**, 81 (1991).
- [37] E. Witten, *Nucl. Phys.* **B249**, 557 (1985).
- [38] R. Jackiw and R. Rossi, *Nucl. Phys.*, **B 190**, 681 (1980).
- [39] M. Hindmarsh, *Physica*, **B 178**, 47 (1992).
- [40] C. Caroli, P.G. de Gennes, and J. Matricon, *Phys. Lett.*, **9**, 307 (1964).
- [41] T.Sh. Misirpashaev and G.E. Volovik, *Physica*, **B 210**, 338 (1995).
- [42] N.B. Kopnin and M.M. Salomaa, *Phys. Rev.*, **B 44**, 9667 (1991).
- [43] N.B. Kopnin, G.E. Volovik and Ü. Parts , *Spectral Flow in Vortex Dynamics of $^3\text{He-B}$ and Superconductors*, cond-mat/9509157, to be published.
- [44] C. G. Callan, Jr., and J. A. Harvey, *Nucl. Phys.* **B 250**, 427 (1985).
- [45] P. Ao and D.J. Thouless, *Phys. Rev. Lett.* **70**, 2158 (1993).
- [46] F. Gaitan, *Phys. Rev.* **B 51**, 9061 (1995).
- [47] S.V. Iordanskii, *Ann. Phys.* **29**, 335 (1964); *ZhETF*, **49**, 225 (1965); [*JETP* , **22**, 160 (1966)].

- [48] E.B. Sonin, *ZhETF* **69**, 921 (1975); [*JETP* **42**, 469 (1976)].
- [49] D. Harari and A.P. Polychronakos, *Phys. Rev.* **D38** (1988), 3320.
- [50] M.G. Alford and F. Wilczek, *Phys. Rev. Lett.* **62**, 1071 (1989).
- [51] A.E. Everett, *Phys. Rev.* **D24** 858 (1981).
- [52] R.L. Davis and E.P.S. Shellard, *Phys. Rev. Lett.*, **63**, 2021 (1989); R.L. Davis, *Physica*, **B 178**, 76 (1992).
- [53] Yu.G. Makhlin and T.Sh. Misirpashaev, *Pis'ma ZhETF* **62**, 74 (1995).
- [54] N.B. Kopnin, *Phys. Rev.* **B 47**, 14354 (1993).
- [55] T.D.C. Bevan, A.J. Manninen, J.B. Cook, A.J. Armstrong, J.R. Hook, and H.E. Hall, *Phys. Rev. Lett.* **74**, 750 (1995).
- [56] W. G. Unruh, *Phys. Rev. D* **51**, 2827 (1995).
- [57] D.V. Gal'tsov and P.S. Letelier, *Phys. Rev.* **D 47** (1993), 4273.
- [58] G.N. Glushchenko, *ZhETF* **104**, 273 (1995); [*JETP* **80**, 145 (1995)].
- [59] N.B. Kopnin, *Physica* **B 210**, 267 (1995).
- [60] G.E. Volovik, *Pis'ma ZhETF* **61** , 935 (1995)
- [61] For a recent paper on this subject, see *Fermion Production in the Background of Minkowski Space Classical Solutions in Spontaneously Broken Gauge Theory*, E. Farhi, J. Goldstone, S. Gutman, K. Rajagopal and R. Singleton, hep-ph/9410365.

Figure Captions

Figure 1: (a) Core of singular vortex or string: Z -string, Abrikosov vortex in superconductor and vortex in neutral superfluid Fermi liquid like ${}^3\text{He-B}$. $f(r)$ characterizes the order parameter or Higgs field. ($f(\infty) = 1$.) The Z -string and the Abrikosov vortex have two length scales: $1/m_{Higgs}$ or coherence length is the scale for the change of the order parameter; while $1/m_Z$ is the penetration length of the magnetic field B_Z of Z -field, which corresponds to the penetration length λ of the magnetic field in superconductor. For electrically neutral superfluid Fermi liquid $\lambda = \infty$. The profile functions $f(r)$ for the unit winding Z -string, Abrikosov vortex and for the $n = 1$ ${}^3\text{He}$ vortex grow linearly with r for small r . (b) Core of the vortex in the A-phase $n = -2$ singular vortex. Note that for this doubly quantized vortex the function $f_1(r)$ is quadratic at the origin.

Figure 2: One of many possible structures of the topological Z_2 soliton in ${}^3\text{He-A}$: the $\hat{\mathbf{l}}$ -soliton. Here the orbital vector $\hat{\mathbf{l}}$ rotates by π in the cross section of the soliton wall (a), while the vector $\hat{\mathbf{d}}$ of the spin part of the order parameter is kept constant (b).

Figure 3: (a) The configuration of the $\hat{\mathbf{l}}$ -field in the isolated continuous vortex with the winding number $n = 2$ in ${}^3\text{He-A}$ (Figure provided by E. Thuneberg). It corresponds to the π_2 charge $\nu_l = 1$ for the $\hat{\mathbf{l}}$ -field. The $\hat{\mathbf{d}}$ -field either has the same configuration ($\nu_d = 1$, dipole locking of $\hat{\mathbf{d}}$ and $\hat{\mathbf{l}}$ fields) or nearly constant ($\nu_d = 0$, the fields $\hat{\mathbf{d}}$ and $\hat{\mathbf{l}}$ are unlocked due to different topological charges). In the typical experimental situations under axial magnetic field, both $\hat{\mathbf{d}}$ and $\hat{\mathbf{l}}$ are perpendicular to the field at infinity. This means that the axial symmetry is broken for such situations. (b) Elementary cell of the periodic vortex structure in the rotating vessel in the regime of low magnetic field (Figure provided by E. Thuneberg). The elementary cell contains $n = 4$ circulation along the cell boundary. (c) Vortex sheet. The $\hat{\mathbf{l}}$ soliton can contain kinks - lines which separate the sections of the soliton with different sense of rotation of the $\hat{\mathbf{l}}$ vector. Each kink represents the vortex with $n = 1$ winding number (first number in the circles). This vortex is however nonsingular $\nu = 0$, since the $\hat{\mathbf{l}}$ -vector also has a winding number around the kink (second number in the circles). Such vortices can live only within the soliton. Under rotation they enter the soliton one by one from the side wall of container and the vortex sheet arises.

Figure 4: (a) Experimental phase diagram of vortex state in the vessel rotating with angular velocity Ω in applied magnetic field. The transition between the vortices with different topological charges is of first order. Due to the high metastability the transition lines are not well resolved. (b) The theoretical phase diagram calculated by E. Thuneberg. The vortex sheet becomes absolutely stable at high rotation velocity.

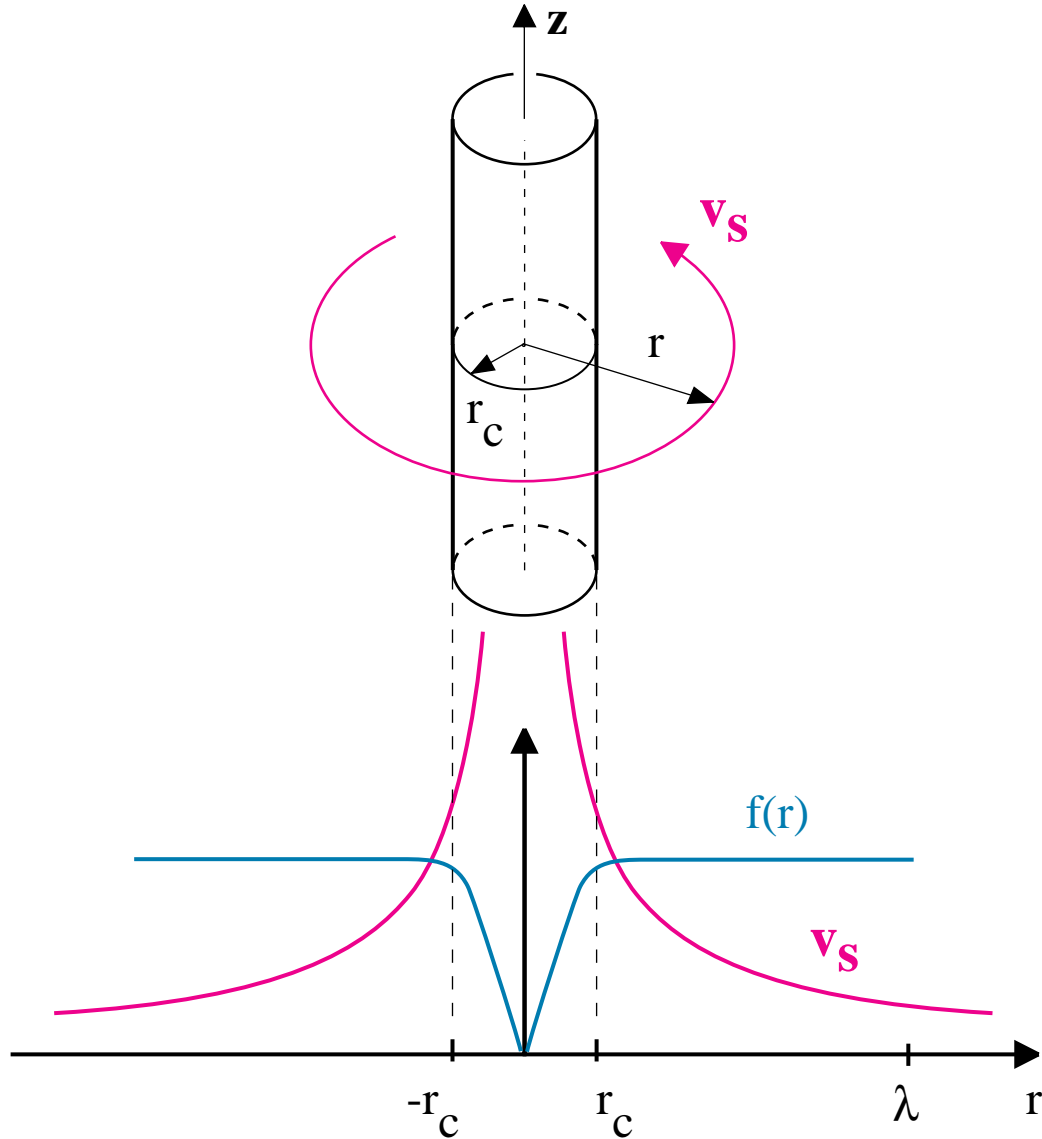
Figure 5: The vortex with $n = 1$ and with constant $\hat{\mathbf{l}}$ -vector at infinity is singular. It contains the hard core within which the order parameter escapes from the vacuum manifold of the ${}^3\text{He-A}$. However practically the whole vorticity $\vec{\nabla} \times \vec{v}_s$ is concentrated outside the hard core in the soft core, where $\hat{\mathbf{l}}$ -vector sweeps the half of unit sphere. (Figure provided by E. Thuneberg)

Figure 6: The transition between the vortices with different topological charges can be mediated by point defects which carry the deficit of the topological charge. The hedgehog in the $\hat{\mathbf{d}}$ field is the interface between the dipole-locked and dipole-unlocked vortices. In the simplest model the interface between the $n = 2$ continuous vortex and two $n = 1$ singular vortices is represented by the hedgehog in the $\hat{\mathbf{I}}$ field, which is similar to the t'Hooft-Polyakov magnetic monopole with physical string.

Figure 7: Transition between the dipole-locked and dipole-unlocked vortices is mediated by hedgehog in the $\hat{\mathbf{d}}$ field. Hedgehog is created on the top or the bottom of the vessel, where the specific point singularity – boojum – always exists as a termination of the continuous vortex (see Ref. [26]). The motion of the hedgehog along the vortex line transforms one vortex to another.

Figure 8: Anomalous branches of fermionic spectrum: (a) fermion zero modes for d and u quarks in Z -string. The massive branches of spectrum correspond to higher values of the generalized angular momentum Q_n . (b-d) In condensed matter vortices the distance between the branches with different Q_n is so small that one can consider this discrete quantum number Q_n as continuous parameter. In this case one has the fermion zero modes in terms of Q_n . The spectral flow along Q_n is responsible for the anomaly in the vortex dynamics which is analogous to the axial anomaly in particle physics. (b) Spectrum of fermions in the $n = 1$ vortex in s -wave superconductor. (c) Spectrum of fermions in symmetric $n = 1$ B-phase vortex looks similar to that in Z -string. (d) Spectrum of fermions in symmetric $n = 1$ A-phase vortex: the branch with $Q_n = 0$ has no dispersion.

String and vortex line with a singular core



core radius r_c

= coherence length ξ in condensed matter vortex

= $1/m_{\text{Higgs}}$ in electroweak string

λ = penetration length of B field in superconductor

= $1/m_Z$ in electroweak Z-string

= ∞ in electrically neutral superfluid ^3He

Fig.1a

Vortex line with a singular core in $^3\text{He-A}$

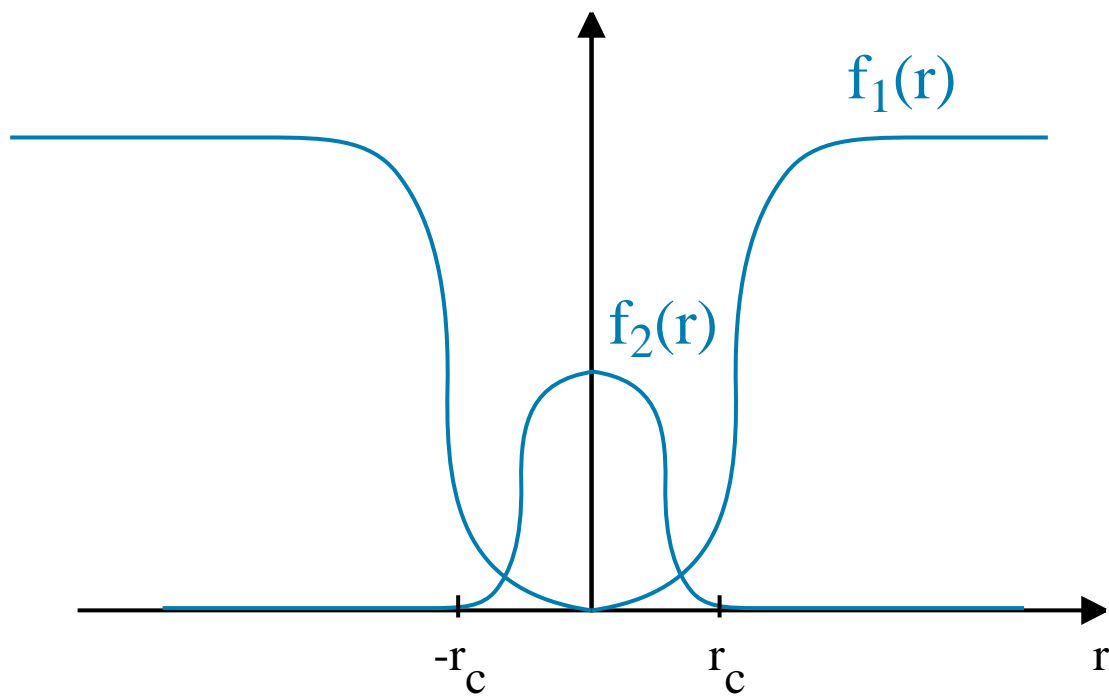


Fig.1b

Soliton in $^3\text{He-A}$

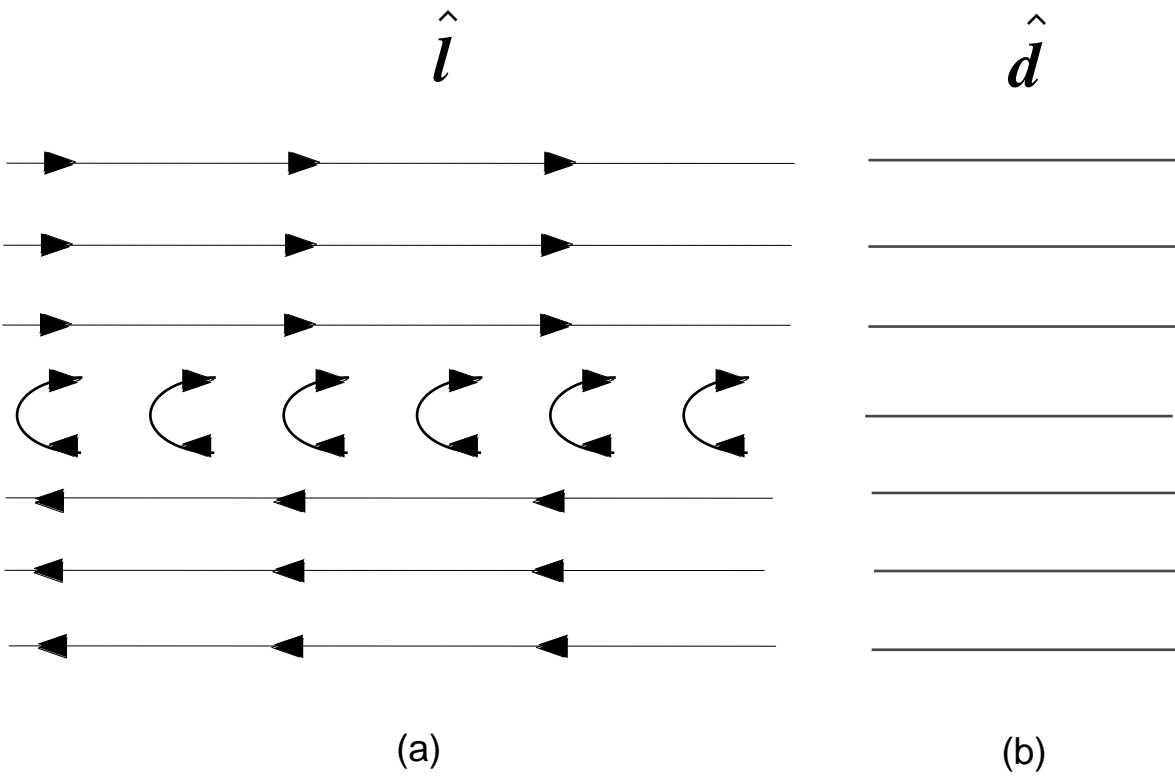
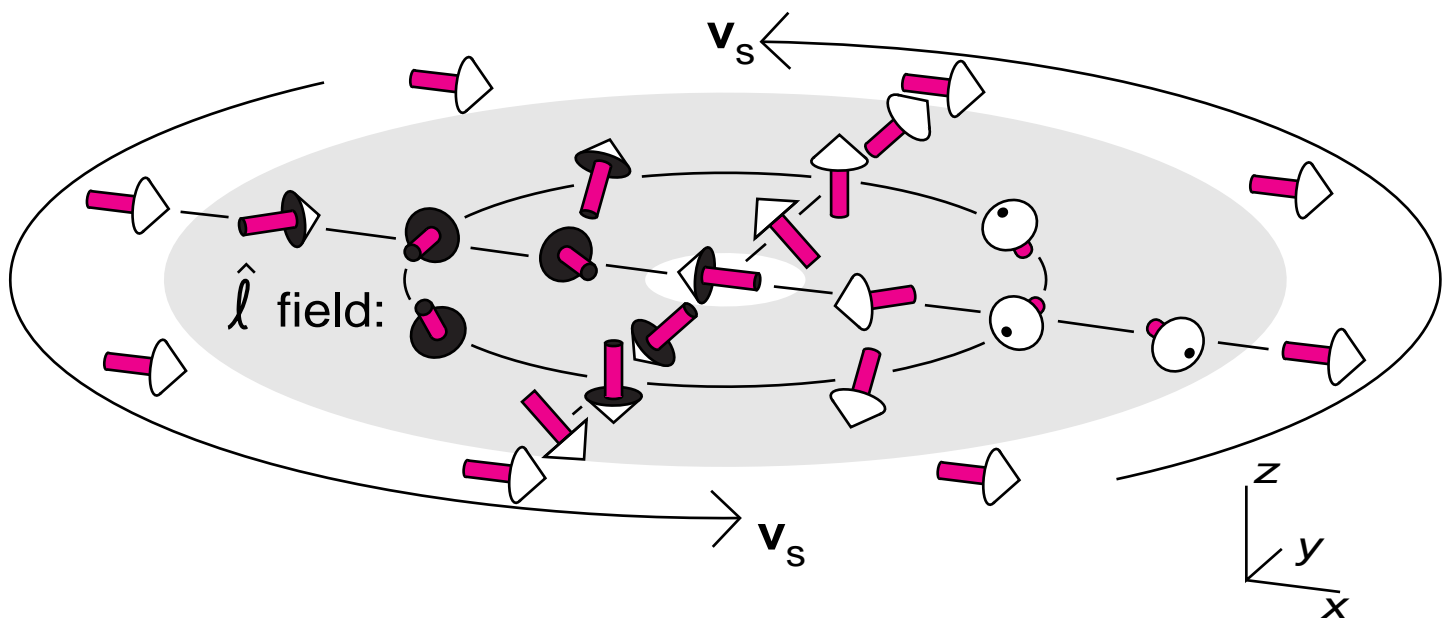


Fig.2

$n=2$ continuous vortices in $^3\text{He-A}$



\hat{d} follows \hat{l} for vortex with $v_l=1, v_d=1$

$\hat{d} \approx$ constant for vortex with $v_l=1, v_d=0$

Fig. 3a

Periodic texture of continuous vortices in rotating container

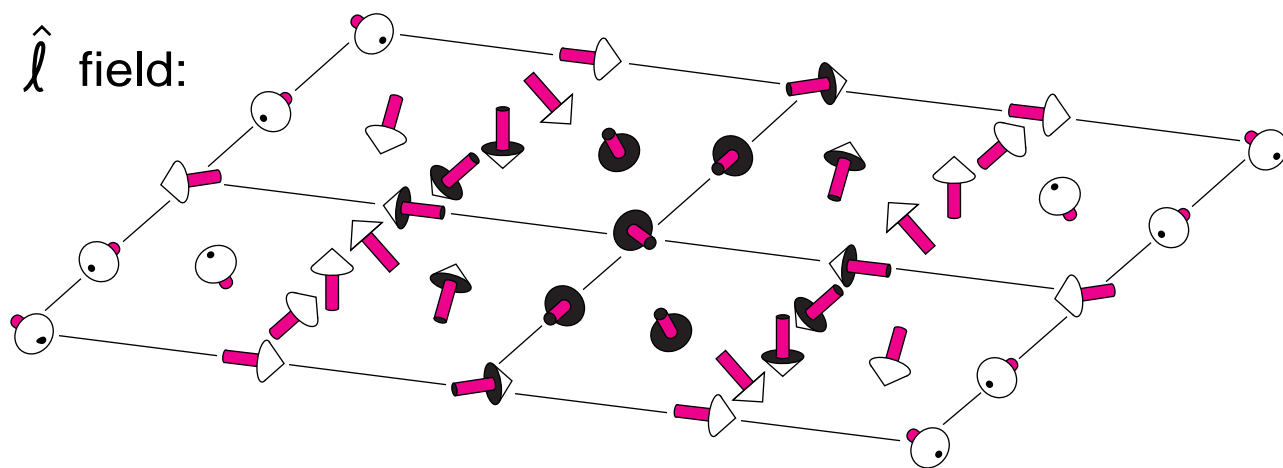


Fig.3b

Vortex sheet: chain of $n=1$ vortices within soliton

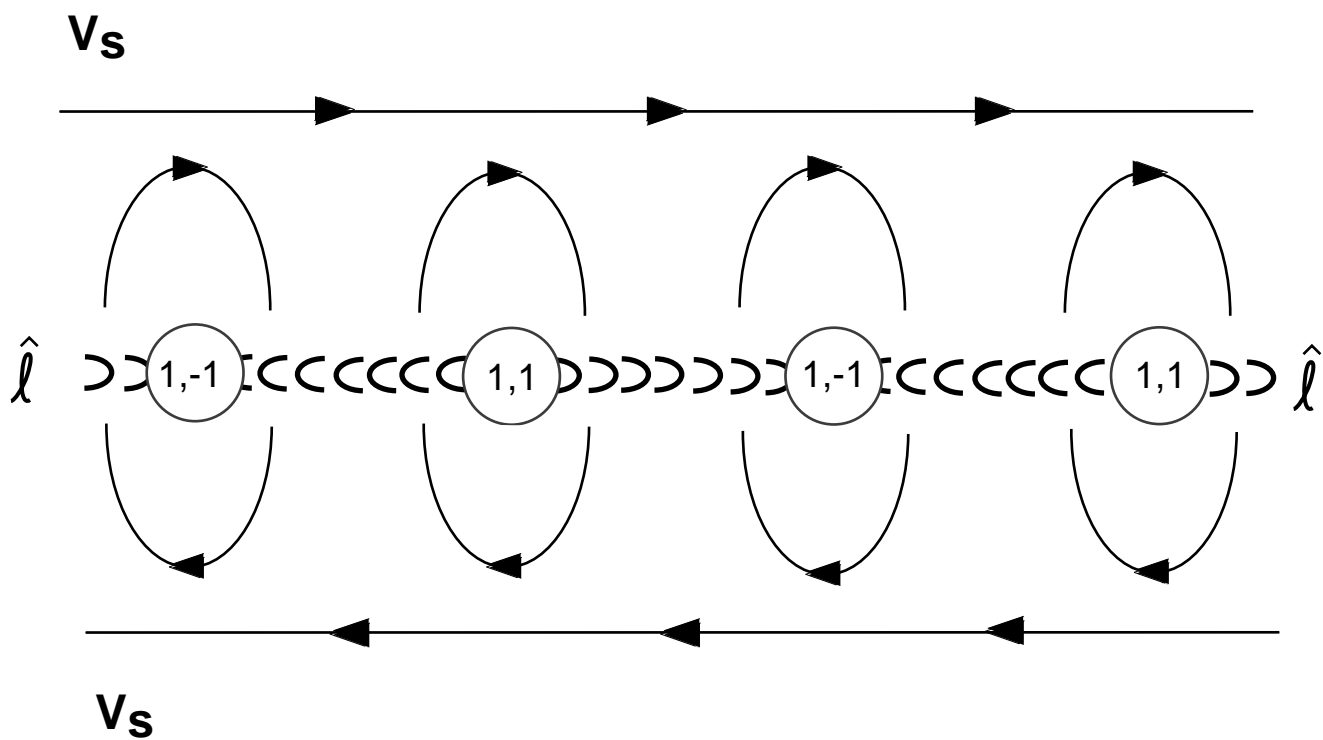
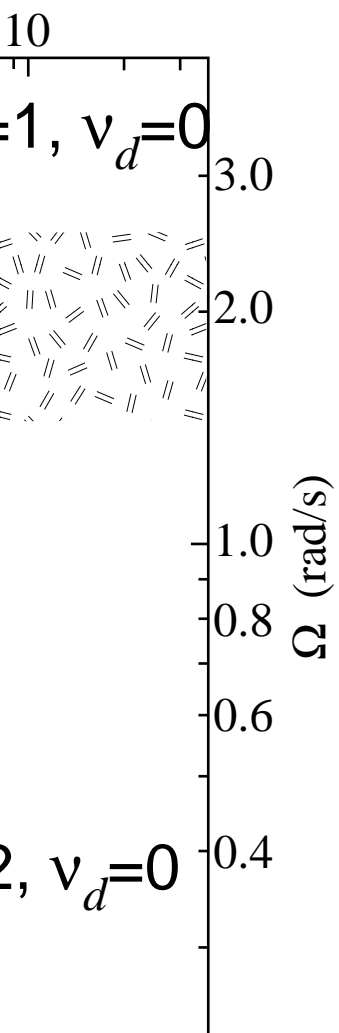


Fig.3c

for ${}^3\text{He-A}$ vortices



Theoretical phase diagram for $^3\text{He-A}$ vortices (E. Thuneberg)

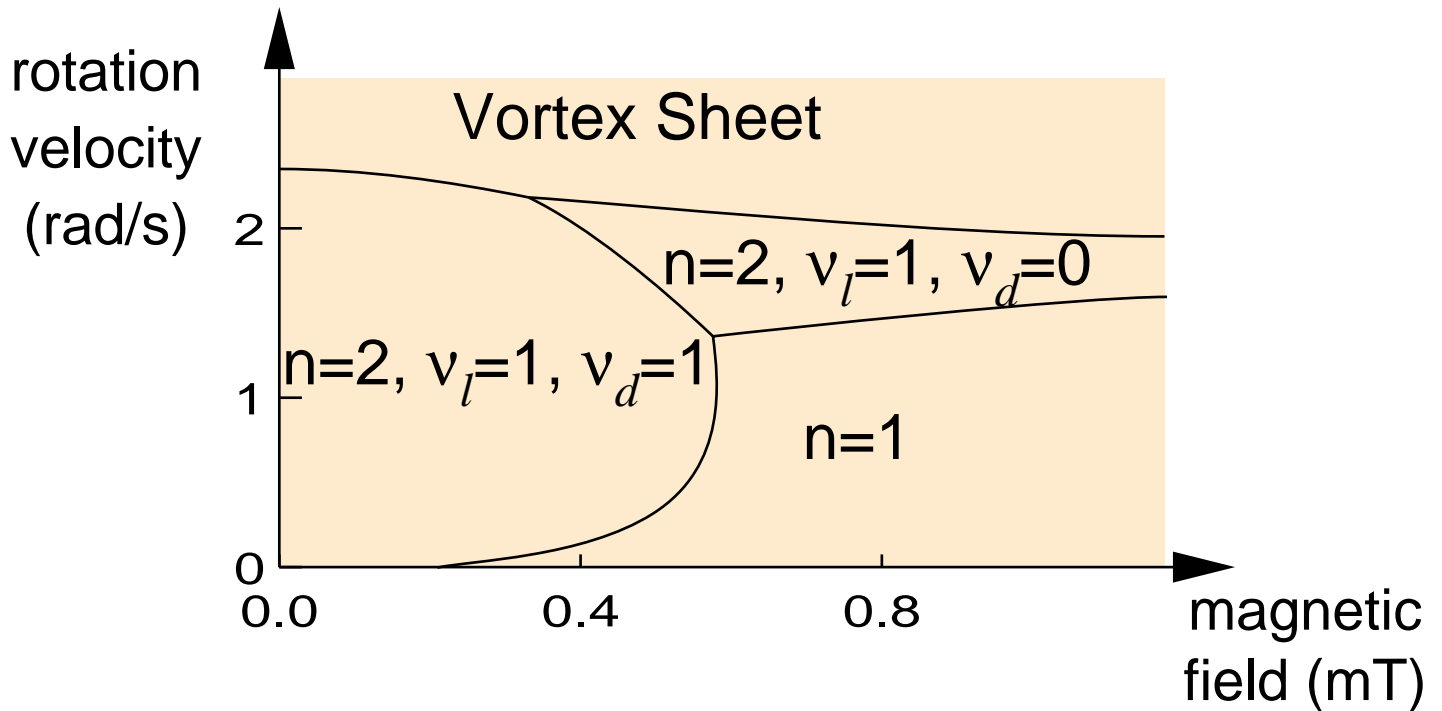


Fig. 4b

$n=1$ singular vortex in ${}^3\text{He-A}$ with $v_l=1/2$, $v_d=0$

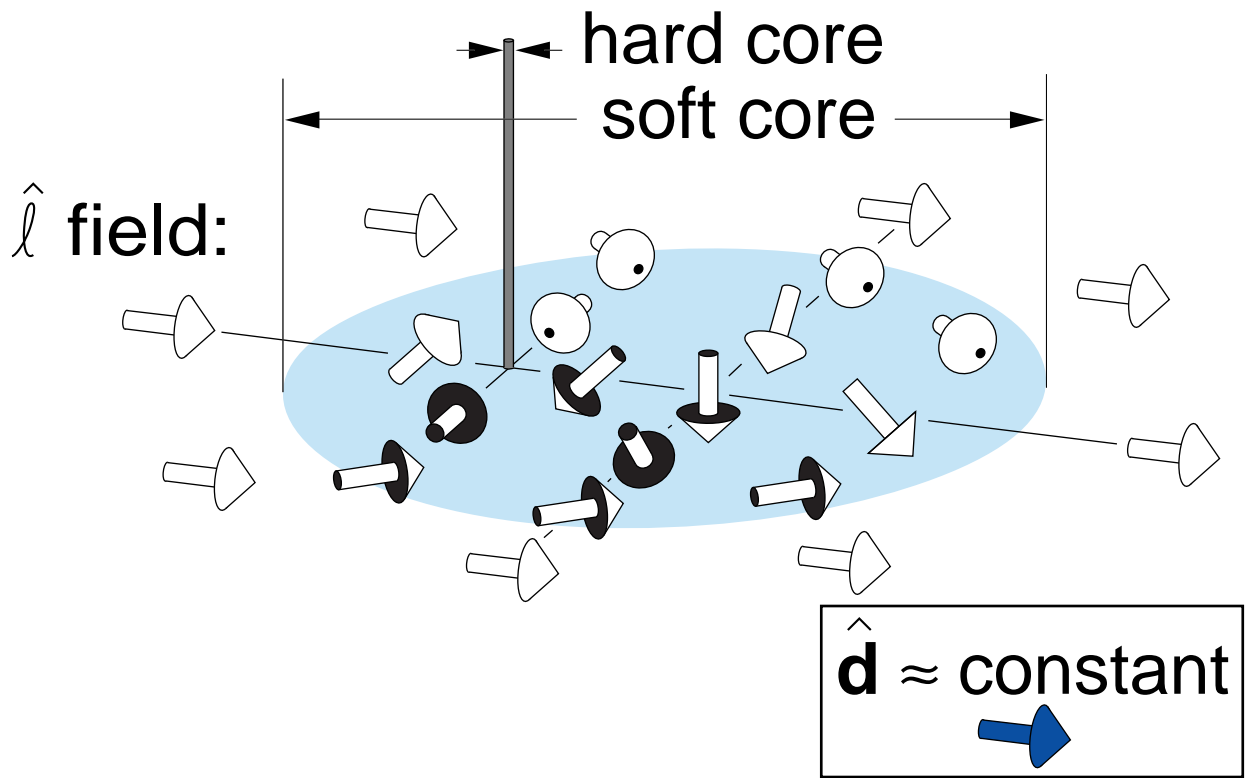


Fig. 5

Hedgehogs: interfaces between different vortex configurations

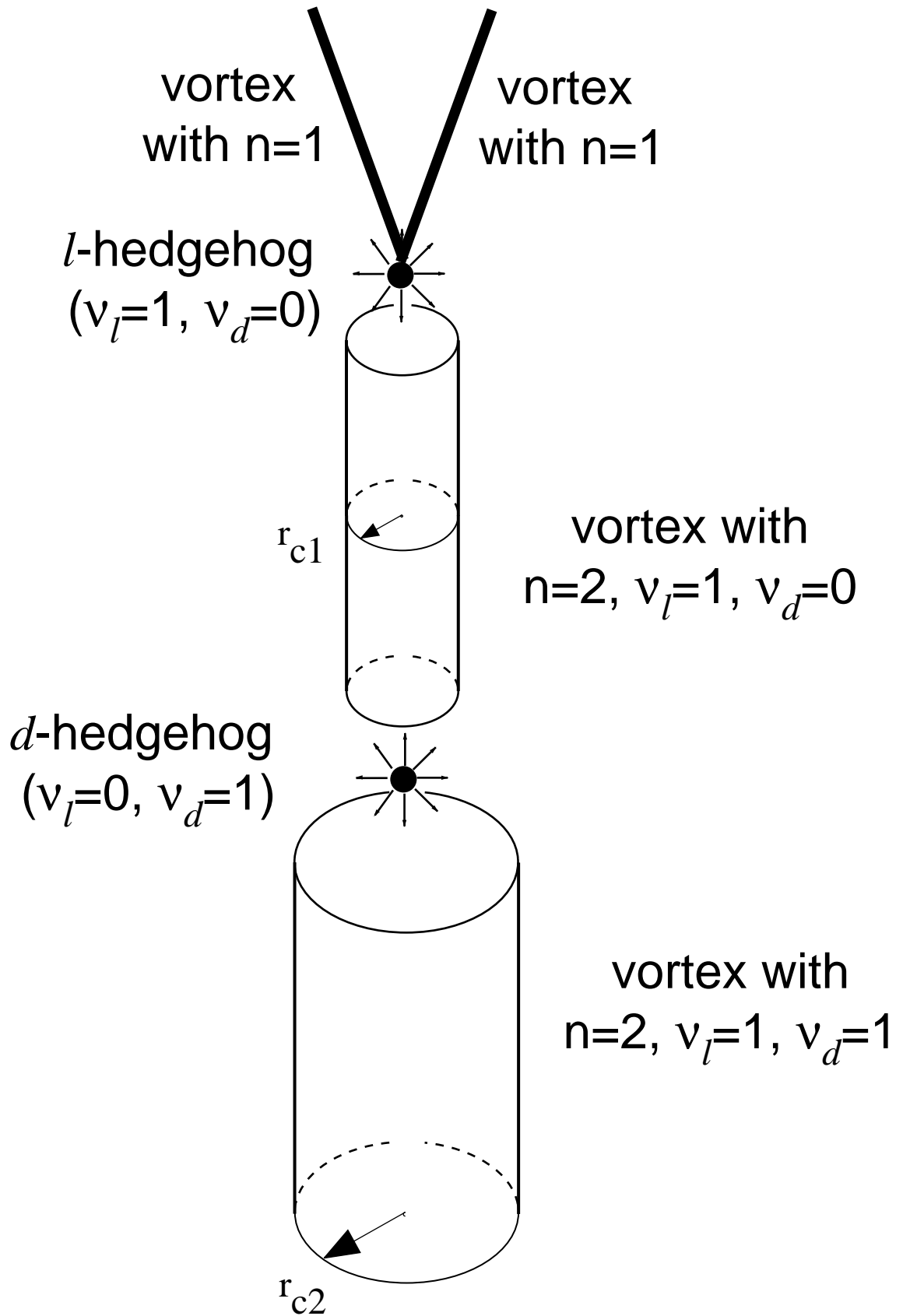


Fig.6

Monopole mediated topological transition between different vortex configurations

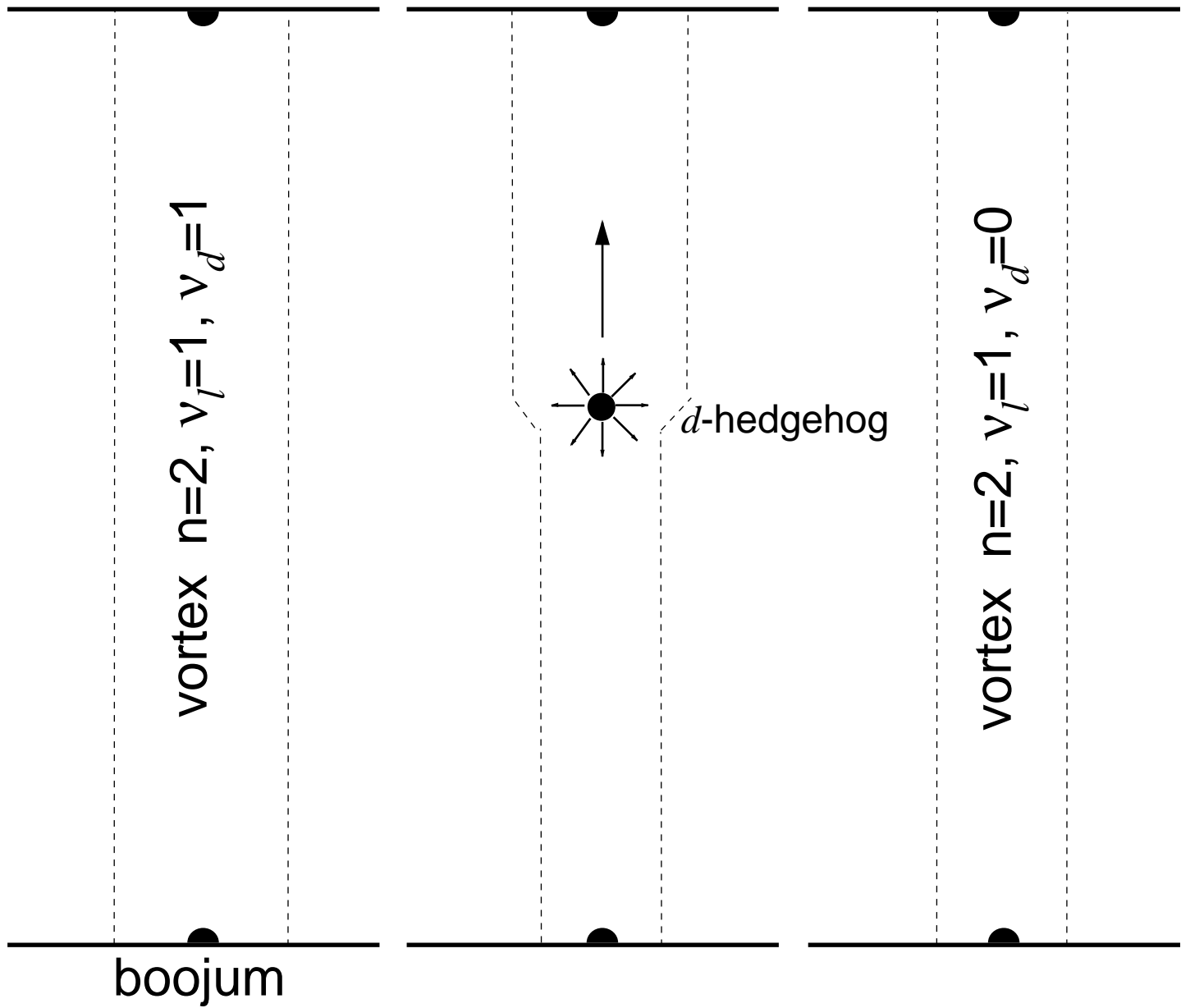


Fig.7

Spectrum of d-quarks and u-quarks in electroweak string

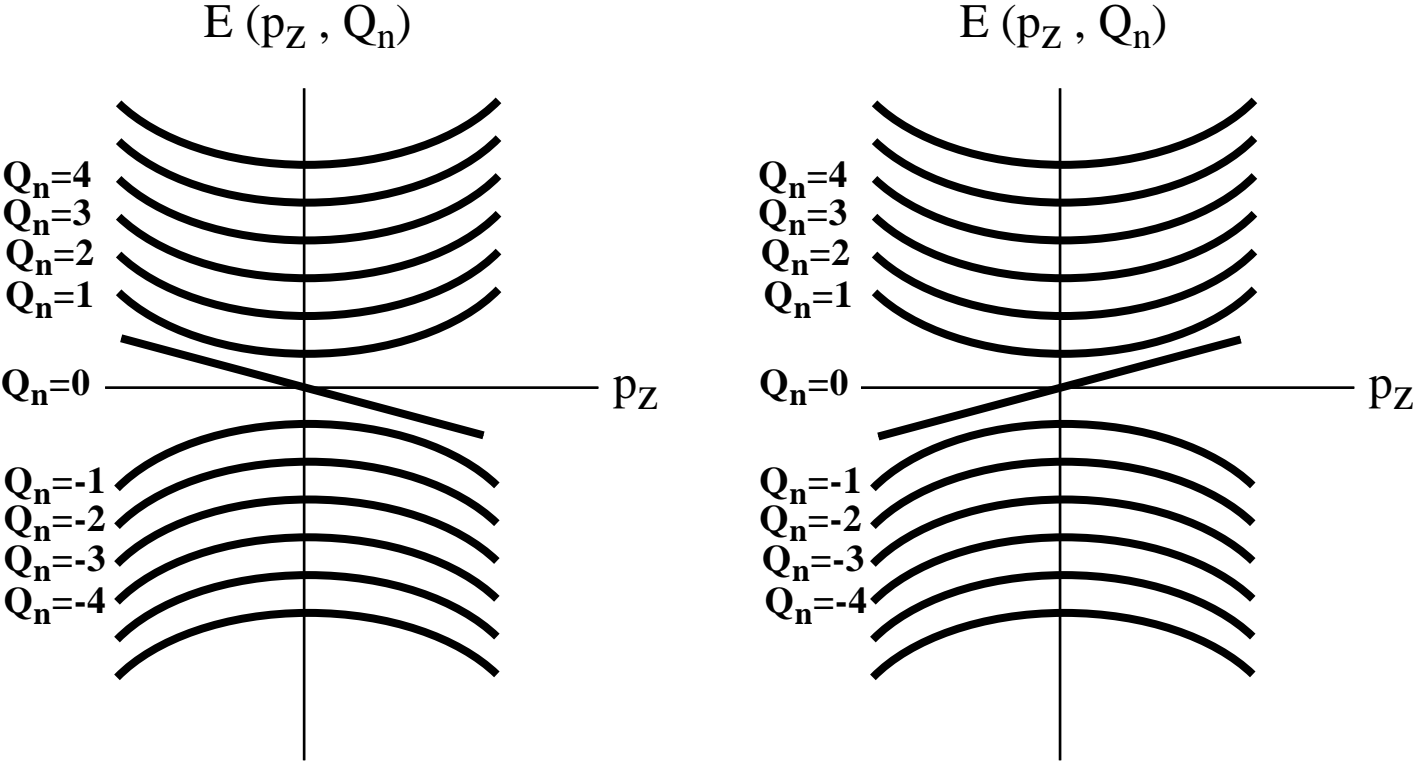


Fig.8a

Spectrum of fermions in vortex in s-wave superconductor.

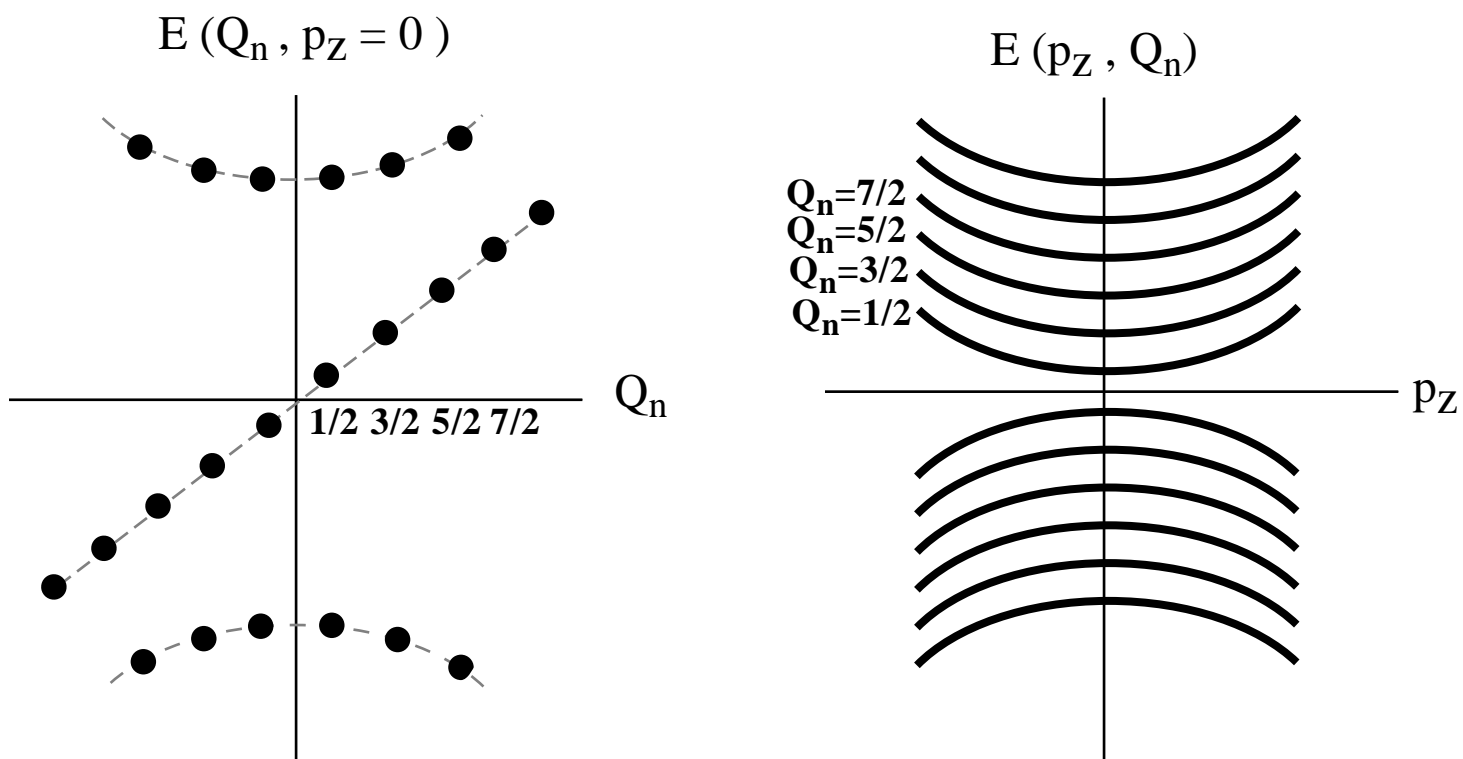


Fig.8b

Spectrum of fermions in symmetric $n=1$ vortex in $^3\text{He-B}$.

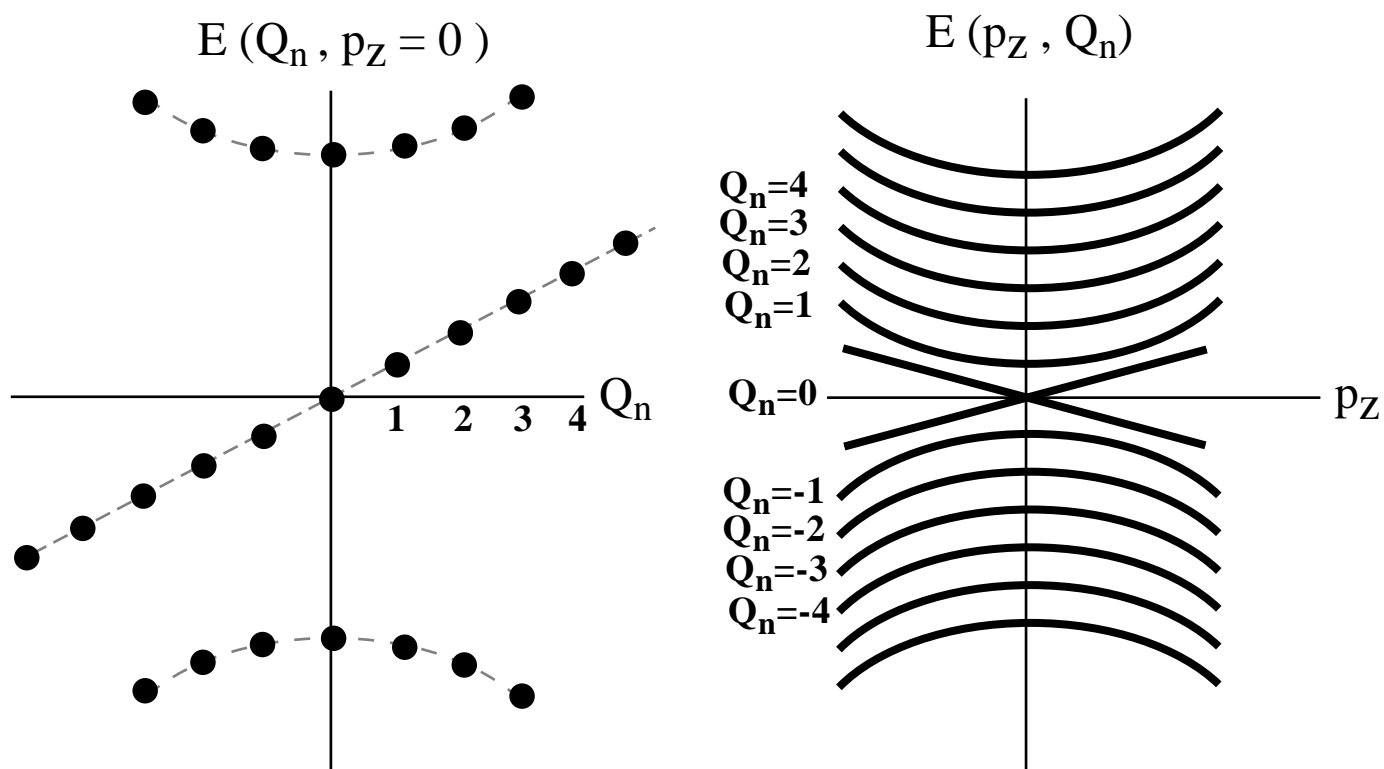


Fig.8c

Spectrum of fermions in symmetric $n=1$ vortex in $^3\text{He-A}$.

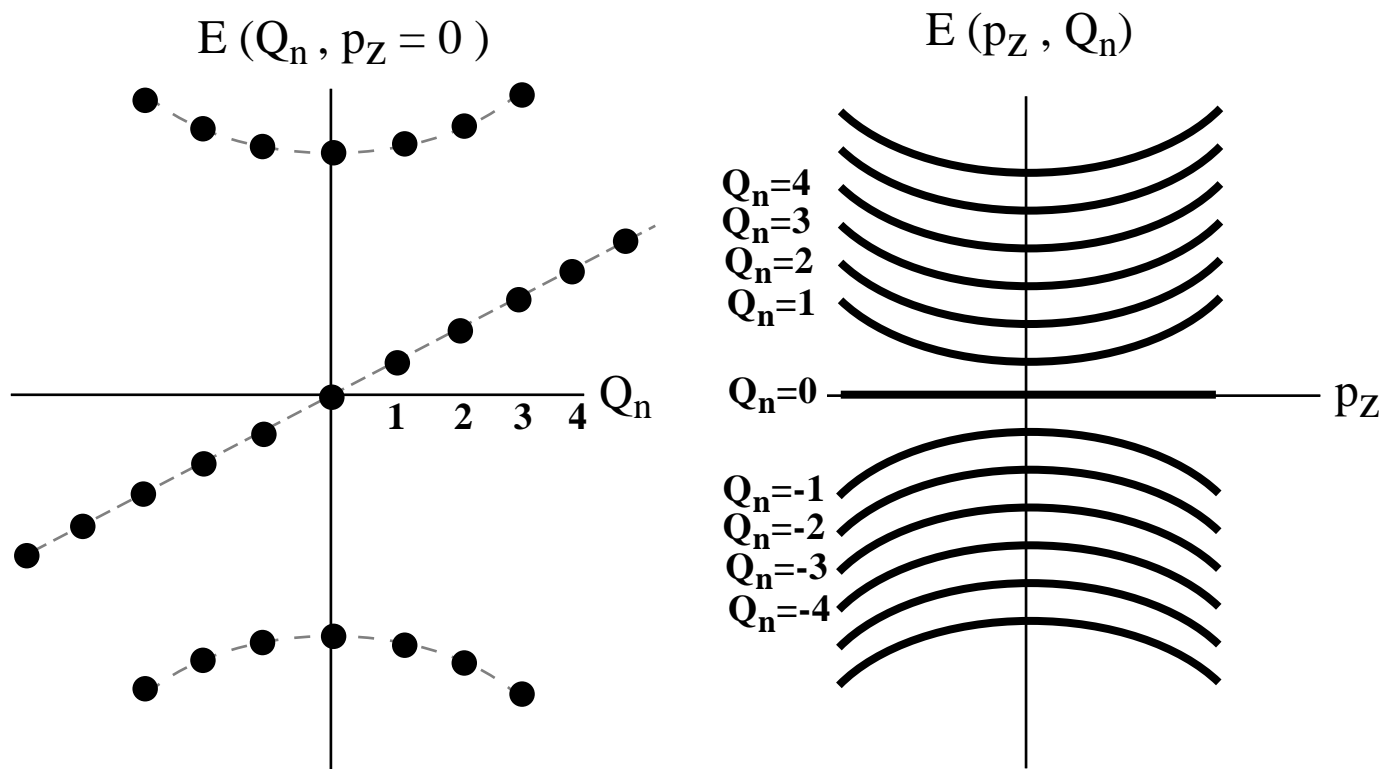


Fig.8d